Static Wheel/Rail Contact

Finite Element Analysis using a parametric modelling approach

B. Bogojević

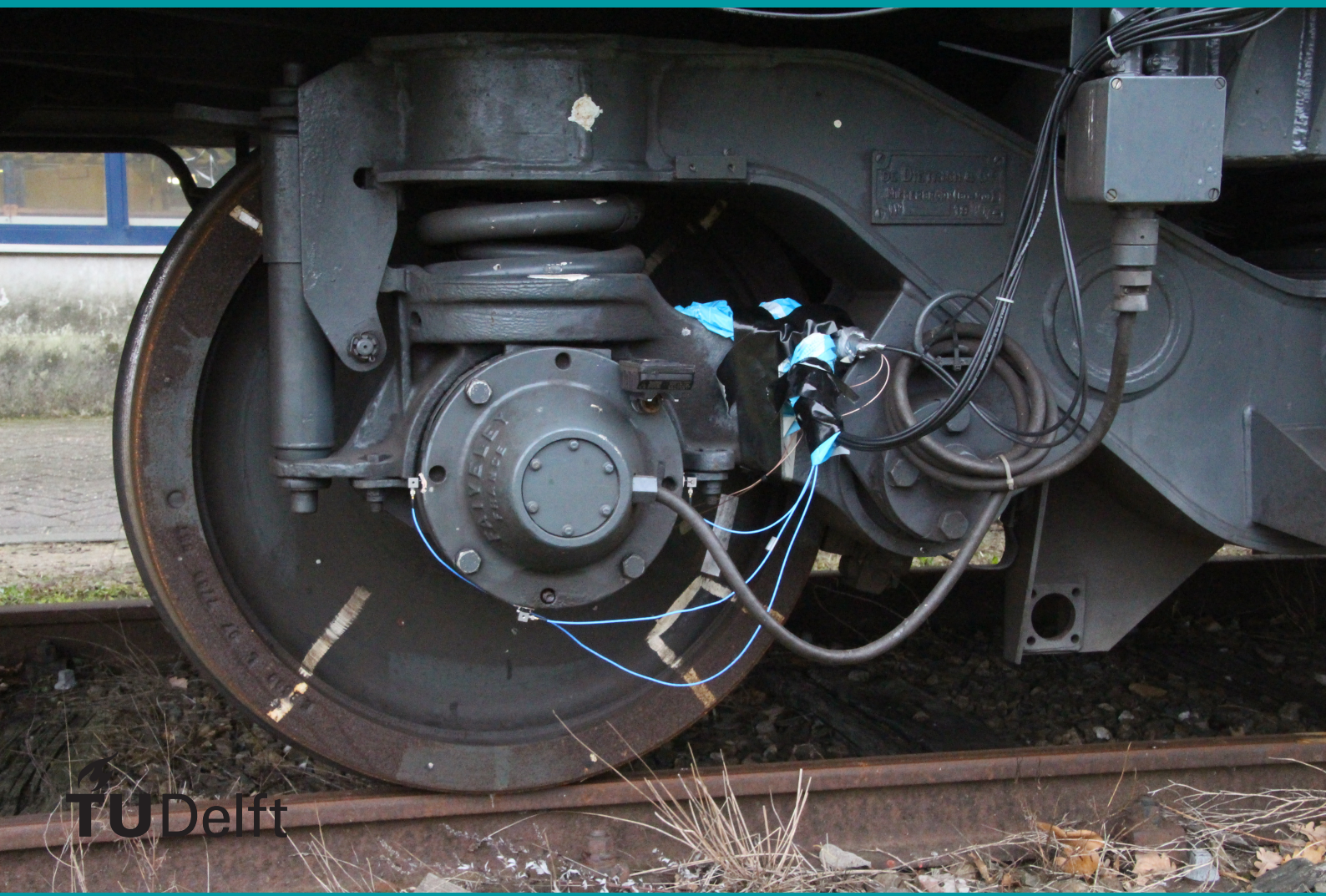

Static Wheel/Rail Contact

Finite Element Analysis using a parametric modelling approach

by

B. Bogojević

to obtain the degree of

Bachelor of Science
in Civil Engineering

at Delft University of Technology,
Faculty of Civil Engineering and Geosciences.

Student number: 4299183
Project duration: September 1, 2017 – October 31, 2017
Thesis committee: Prof. dr. ir. Z. Li, TU Delft, supervisor
Dr. ir. Z. Qian, TU Delft, supervisor

TU Delft

Contents

1 Introduction

1.1. Problem context

Railways are complex dynamic systems. Infrastructure and rolling stock need to be integrated very well to provide fast, safe and reliable rail transport. The way the vehicle interacts with its driveway is unique to this mode of transportation.

The interaction between a train and track takes place through the wheel-rail interface. Both the wheels and rails are made of steel. Although they are both hard, they are still deformable as the load of the train and its passengers or freight on the rail is quite high. The contact between wheel and rail, material characteristics and loads are key to many problems such as wear, rolling contact fatigue and damage. As a result, the problem context can be formulated as follows:

> *Wheel-rail interaction is a fundamental and crucial element for successful railway transportation. Large forces transmitted in the wheel-rail interface in combination with material and dynamic characteristics cause high stresses and can eventually lead to problems.*

1.2. Research objectives

It is important to know the contact profile and stresses in order to contribute to a solution for the wheel-rail contact problem. The ability to compute contact profile and stresses, can lead to future designs of wheels and rails which perform better (e.g. increased speed, reduced noise or less wear/damage). In this context, the main objective of this research can be identified as follows:

> *Propose a realistic model of wheel and rail interaction from which the contact profile and stresses in the wheel and rail in static conditions can be derived.*

1.3. Research questions

The previous stated research objective is successfully achieved if it provides an answer to the proposed research question below. The main research question is:

> *What is the contact profile and what stresses occur in the wheel and rail?*

In order to answer the main research question, the following sub questions need to be addressed first.

1. *What is the wheel/rail contact problem?*
2. *How does the wheel/rail contact problem influences railway operation?*
3. *How can Finite Element Analysis be used to model wheel/rail contact?*
4. *What are the differences between the solution of FEA and the analytical solution?*

1.4. Methodology

A Finite Element model is proposed to answer the main research question. It is build in the ANSYS® Mechanical Advanced Programming Design Language™ (MAPDL) environment. The way a Finite Element Method (FEM) model is fundamentally created, results in poor adaptability of the model once it is build. Therefore small changes cannot be made without a great investment of time effort to almost completely rebuild the model. Since there a many variables applicable in this (and future) situation(s), a parametric modelling approach is used.

1.5. Thesis structure

In chapter 2 an introduction to the wheel/rail contact problem and its influence on its surrounding and railway operation is given. Furthermore, the problem will be mathematically described with the used of the Hertz contact theory. In chapter 3 Finite Element Analysis is described and the proposed model is presented. In chapter 4 the solution of the FEM model is validated. Chapter 5 will sum up the outcome of this research and give a recommendation for future research.

2

The wheel-rail contact problem

2.1. Historical perspective of wheel/rail contact

The first railway system like it is known today, by using coned flanged wheels and cast iron (steel nowadays) rails, was invented in the 1830s during the industrial revolution. The British railway pioneers George Stephenson and Isambard Kingdom Brunel were the first who explained the self-steering mechanism due to coned wheels and build the first operational steam locomotive [10]. The first railway line in the Netherlands opened in 1839 between Amsterdam and Haarlem [12].

During the 1800s, trains were mostly powered by steam and operational speed was normally not exceeding 50 km/h. Typical axle load at this time was around 10 tonnes. Ever since, technology evolved and demands of railways increased. Today, most trains are diesel or electric powered and axle loads of 22,5 tonnes (in the USA sometimes even 30) are standard. The maximum speed on regular tracks increased to 140-160 km/h [10].

Although steam trains were already running all over the world in the 1880s, the first railway engineering related scientific breakthroughs occurred in this period. Physicist Heinrich Hertz is nowadays well known for his fundamental work in different fields of physics. In his scientific paper published in 1881, he mentions the wheel-rail contact problem [4] and his theory of elastic contact mechanics was soon found very well application in railway engineering. Assumptions based on Hertzian contact models are still very common in research and analysis of the wheel-rail interface [10, 13].

Nowadays, it is not only due to higher speeds and axle loads the more demanding conditions for the wheel-rail interface exist. Numerical computer simulations, control and safety systems all have invaded railway engineering and have led to refined traction control and braking [10]. This caused better performance of the wheel-rail interface, but also introduced a set of new problems.

2.2. Phenomena due to the wheel-rail interface

The wheel-driveway interaction of railways is very different from other ways of transportation over land like seen on roads for instance. The biggest difference is the use of hard surfaces in the contact region of both the vehicle and driveway (rail for railways). This results in a very small contact patch, low rolling contact losses and thus high energy efficiency. This sounds ideal, but a small contact patch introduces several undesired phenomena as seen in Figure 2.1.

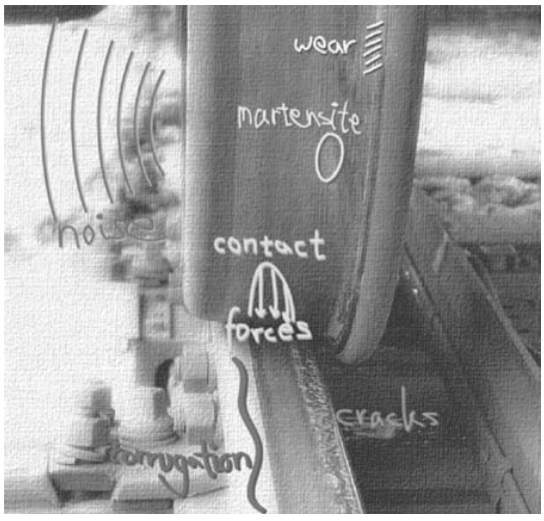

Figure 2.1: Phenomena due to wheel/rail contact (picture from [10])

High contact forces in vertical, lateral or longitudinal direction result in high stresses that may cause yielding and/or fatigue of both wheel and rail. These forces combined with friction are the main reason for wear. Traction and braking can lead to sliding resulting in rail burns and wheelflats. These undesired phenomena are a result of the small contact interface leading to irregularities and disturbed geometries of wheel and rail.

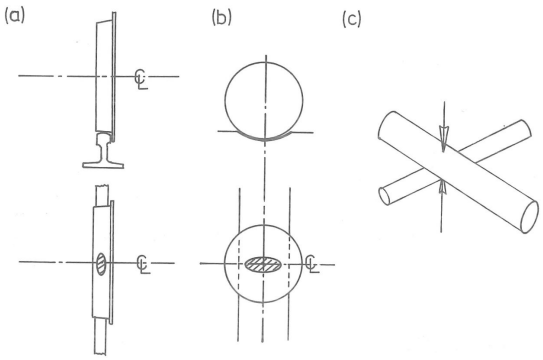

Figure 2.2: Examples of general elliptical Hertizan contact: (a) Coned railway wheel on rail (b) Ball rolling in a nonconforming groove (bad ball bearing for instance) (c) Two crossed cylinders with varying diameters (figure obtained from [5])

Although these irregularities are mostly dealt with by suspension systems, bogie designs and other measures, poor vehicle dynamics and further increase of contact forces (and thus faster/worse geometry deterioration!) and noise generation still occur. Passenger discomfort and railway surrounding area disturbance are a consequence. To keep these consequences to a minimum maintenance to wheels, rails and other components are needed and thus require an economical investment. Extreme cases of irregularities like rail fracture or wheel flange climbing onto the rail can even result in serious accidents like derailment.

2.3. Hertzian contact theory

A general Hertzian contact occurs whenever the surfaces of two bodies in contact can be described by second order expressions [5]. The dimensions of the contact area are small in comparison to the bodies and radii of curvature of the bodies involved. Some examples can be as seen in Figure 2.2. Contact between two cylinder-like bodies result in an elliptical shaped contact patch, where the major axis is aligned with the direction of rolling. The first step in solving the contact problem is finding the principal axes lying in the plane of contact such that the term xy vanishes in the following equation [3, 8]):

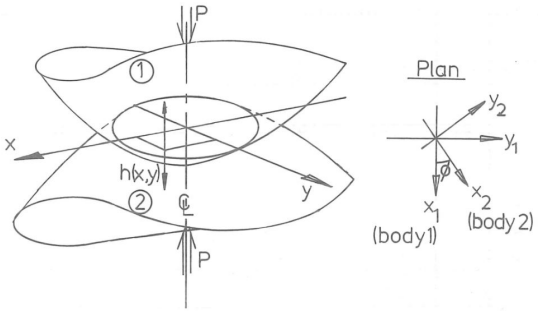

Figure 2.3: Geometry of two cylindrical contacting bodies with a load P applied to them (figure obtained from [5])

$$h(x,y) = \frac{1}{2}Ax^2 + \frac{1}{2}By^2 + \frac{1}{2}Cxy \tag{2.1}$$

where h is the relative separation of point at initial contact (as seen in Figure 2.3).

Greenwood, Johnson have stated that the coefficients A and B are directly related to the radii of curvature of the bodies involved:

$$A+B = \left(\frac{1}{R_1} + \frac{1}{R_1'} + \frac{1}{R_2} + \frac{1}{R_2'}\right) \tag{2.2}$$

$$A-B = \left[\left(\frac{1}{R_1} - \frac{1}{R_1'}\right)^2 + \left(\frac{1}{R_2} - \frac{1}{R_2'}\right)^2 + 2\left(\frac{1}{R_1} - \frac{1}{R_1'}\right)\left(\frac{1}{R_2} - \frac{1}{R_2'}\right)\cos 2\phi\right] \tag{2.3}$$

$$C = 0$$

where R_1 and R_1' are the principal rolling and principal transverse radius respectively of body 1, R_2 and R_2' are the principal rolling and principal transverse radius respectively of body 2 and ϕ is the relative angle between the normal planes of both bodies. Note that the radii are considered positive if the surface is convex (centerpoint lays 'inside' the body).

The contours of initial separation (Equation 2.1) are seen to be ellipses whose semi-axes have a ratio of $\sqrt{B/A}$ [4], and we assume at this point that the contact patch will be an ellipse as well, with semi-axes of length a and b. Also assumed it that the pressure distribution is in the form of an ellipsoid (see Figure 2.4), i.e. the pressure distribution is described by

$$p(x,y) = -p_0\sqrt{1-(x/a)^2-(y/b)^2}, \tag{2.4}$$

which can be found over the assumed elliptical shaped contact patch

$$\left(\frac{x}{a}\right)^2 + \left(\frac{y}{b}\right)^2 \leq 1. \tag{2.5}$$

Proof that these two assumptions are indeed correct, can be found in [5].

Since we assumed the ellipsoidal stress distribution is correct, the integration of the contact pressure over the contact ellipse should be equal to the applied load P, resulting in

$$p_0 = \frac{3P}{2\pi ab} \tag{2.6}$$

where p_0 is the maximum contact pressure (see Figure 2.4).

Since the load P is known are can be measured relatively easy, the only question remaining is what are the dimensions of the elliptical contact patch? I.e. what are the values of semi-axes a and b? These values can be derived from the Hertzian contact theory [2, 4] where

$$a = m[3\pi P(K_1 + K_2)/4K_3]^{1/3}, \tag{2.7}$$

$$b = n[3\pi P(K_1 + K_2)/4K_3]^{1/3}, \tag{2.8}$$

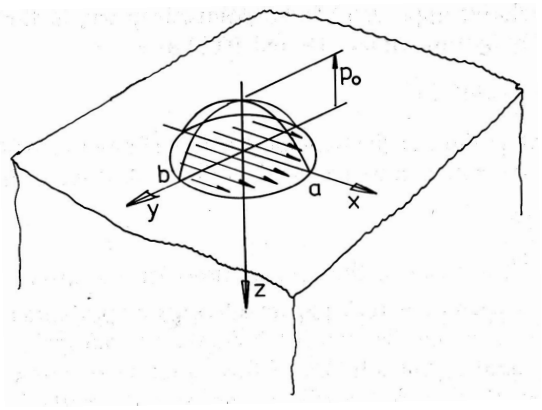

Figure 2.4: Contact pressure distribution on a elastic half space $z > 0$ (figure obtained from [5])

The semi-axes are depending of k-values, which are defined as:

$$K_1 = \frac{1-\sigma_W^2}{\pi E_W}, \qquad K_2 = \frac{1-\sigma_R^2}{\pi E_R}, \tag{2.9}$$

$$K_3 = \frac{A+B}{2}, \tag{2.10}$$

where σ_W and σ_R are the Poission's ratio for the wheel and rail respectively, E_W and E_R are the Young's modulus of elasticity of the wheel and rail respectively.

If we substitute (2.2) into (2.10) we obtain

$$K_3 = \frac{1}{2}\left(\frac{1}{R_1} + \frac{1}{R_1'} + \frac{1}{R_2} + \frac{1}{R_2'}\right). \tag{2.11}$$

Determining the coefficients m and n are part of a complex part of the solution to the general Hertz contact problem. These require to solve two complete elliptic integrals and there have been numerous papers offering an approximate solution to this problem [5]. Tabulated approximate solutions are for instance provided by [9, 11]. Figure 2.5 shows values of θ and the corresponding values for m and n.

θ =	30°	35°	40°	45°	50°	55°	60°	65°	70°	75°	80°	85°	90°
m =	2.731	2.397	2.136	1.926	1.754	1.611	1.486	1.378	1.284	1.202	1.128	1.061	1.000
n =	0.493	0.530	0.567	0.604	0.641	0.678	0.717	0.759	0.802	0.846	0.893	0.944	1.000

Figure 2.5: Values of m and n depending on θ (table obtained from [11])

As seen in Figure 2.5, m and n are dependent on θ. The value of θ can be obtained by

$$\theta = cos^{-1}(K_4/K_3) \tag{2.12}$$

where

$$K_4 = \frac{A-B}{2}. \tag{2.13}$$

Substitution of (2.3) into (2.13) results into

$$K_4 = \frac{1}{2}\left[\left(\frac{1}{R_1}-\frac{1}{R_1'}\right)^2+\left(\frac{1}{R_2}-\frac{1}{R_2'}\right)^2+2\left(\frac{1}{R_1}-\frac{1}{R_1'}\right)\left(\frac{1}{R_2}-\frac{1}{R_2'}\right)\cos(2\phi)\right]. \tag{2.14}$$

At this point, the wheel rail contact problem is simplified and mathematically described. With the use of the approximate values for m and n as seen in Figure 2.5, an analytical solution can be obtained which later in this report will be used for validation of the FEM model.

3

Modelling the wheel-rail contact problem

3.1. The Finite Element Method

The Finite Element Method (FEM), also known as Finite Element Analysis (FEA), is a computational method to solve boundary value problems whereby the obtained solution is an approximation. A boundary value problem is a mathematical problem in which dependent *field* variables must satisfy a differential equation everywhere in a predefined domain and specific conditions on the boundaries of this domain. Since the domain and its boundary conditions can be defined any way desired, FEM is often used for mathematics or engineering whereby the domain often represents a physical structure. Depending on the type of physical problem, the field variables can be e.g. displacement, temperature, heat flux, etc [7].

A volume of some material with known physical properties can be seen in Figure 3.1a. The volume represents the domain of a boundary value problem. For simplicity a two-dimensional case with one field variable is assumed. The field variable needs to be determined at every point P(x,y) such that a known (differential) equation is satisfied here. This implies an exact mathematical solution is solved for. In practical problems, the geometry of the domain can be very complex why obtaining an exact closed-form solution is very difficult or even impossible. Therefore, approximate solutions based on numerical computation are often used in complex problems. This makes Finite Element Analysis is a powerful tool for obtaining approximate solutions with good accuracy in a relative small amount of time [7].

A small triangular element that represents a part of the domain is shown in Figure 3.1b. This element is not an often used differential element of size $dx \times dy$, but it has physical dimensions. This makes it a finite element and this is also where the name of this method comes from. The vertices of the element are numbered, these points are so called nodes. Nodes are specific points in a finite element at which the field variable is calculated. There are two types of nodes:

1. **Exterior nodes**
   These nodes are located on the boundaries of the finite element and can be used to connect an element to adjacent finite elements. The finite element shown in 3.1b has only exterior nodes.

2. **Interior nodes**
   Nodes that do not lie on element boundaries are interior nodes and cannot be connected to any other element. This type of nodes can be used to decrease interpolation error and thus increase accuracy.

As said before, the values of field variables are computed only at nodes. The power of FEM is found in how field variables are obtained at any other points in the finite element: the field variable computed at the nodes are used to approximate the values at other points by interpolation of the nodal values. In this manner, a approximation of every single point in the domain can be obtained by only explicit calculating the field values of the field variables at nodes [7].

Elements can be defined with different shapes and properties. It is possible to define your own element shape and properties, but since there are many similar problems to be solved does FEM software often comes with predefined element *types*. Different physical problems can benefit from a different element types. For instance, a structural problem only consisting of a loaded solid beam, can be modelled by brick elements, with 8 exterior nodes on all vertices for instance. But if the solution is not satisfying, a 20 node brick with

extra interior nodes can be used. For contact problems, there are different elements necessary to model the contact between two bodies. Non-linear spring-damper behaving elements can be used, or a simple linear spring model depending on the computational time and physical problem.

This element-based approach is used to cover the whole predefined domain. As seen in Figure 3.1c, every element is connected at its exterior nodes to other elements. The finite element equations are such formulated that at the nodal connections, the field variable has the same value for each element connected to the node. This results in continuity of the field variable at the nodes. A side-effect of this way of defining the finite element equations is that continuity of the field variable across element boundaries is also ensured. This feature avoids gaps or voids between elements in the solution of the boundary value problem [7].

The procedure for creating a FEM model has (generally speaking) three phases:

1. Preprocessing
2. Solving
3. Postprocessing

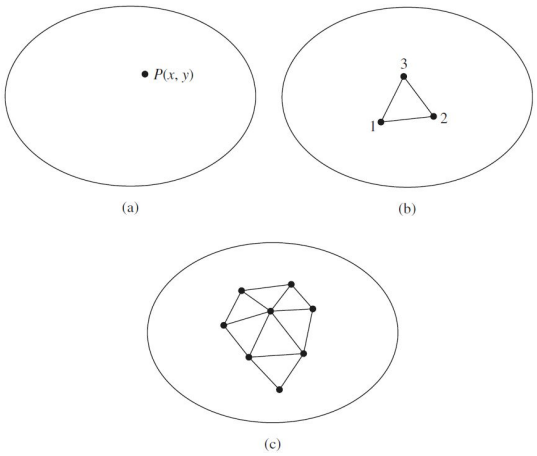

Figure 3.1: (a) A general two-dimensional domain of any field variable. (b) A three-node finite element. (c) Additional elements showing a partial finite element mesh of the domain. (figure obtained from [7])

Preprocessing In the preprossessing phase, all physical properties and computational settings are assigned to the model. Think of defining:

- Geometric domain (often called geometry)
- Element type(s)
- Material model/properties
- Geometric element properties (dimensions)
- Element connections (meshing)
- Boundary conditions (physical constraints)
- Load applied to the geometry
- Specify solver properties

Solving If the model is defined correctly in the preprocessing phase, the software assembles all algebraic equations in matrix form and computes the values of the field variable(s) iteratively during the solving phase.

Postprocessing In the postprocessing phase, all analysis and evaluation of the solution is done. The solution can be sorted, printed or plotted. Some other operations that can be done in this stage:

- Check equilibrium (verify if the solution is realistic)
- Plot deformed structural shape
- Plot distribution of field variable(s)
- Animate dynamic loading and/or model behaviour

The solution data can be used in may ways during postprocessing, but the most important objective is determining whether the results are physically possible and reasonable [7].

3.2. The proposed model

3.2.1. The modelling approach

The conventional approach by manual modelling using the Graphic User Interface (GUI) results in a permanent model whereby changes often need to be implemented by deleting a whole section and redefine it again. This can be particular time consuming if a change needs to be made in the geometry for instance, since besides the new geometry, the mesh needs to be redefined as well. A simple change can result in a very time consuming operation.

The proposed model is build differently, by using a parametric modelling approach. By this approach, the model is created by a script (called a *macro*) whereby parameters are used. This results in a highly adaptive model without the need for manual processing changes since the model can rebuild itself by following the macro. Also future improvements or additions to the model can be easily processed by simple adding these changes or features to the macro and let the model rebuild itself. This costs only a fraction of the time compared to manual processing. This approach has disadvantage though: it requires to create the macro as such, that is as independent of other elements in the model as possible. Example: when extruding an area into a volume, it should not be dependent on the position or geometry of the area to be extruded. This process requires more time compared to build it via an GUI since beforehand there needs to be thought of the independent definition/implementation. In Table 3.1 a direct comparison of both methods is made. Please note that it is compared relative to each other.

Table 3.1: Conventional and parametric modelling compared

	Conventional/GUI	Parametric
Adaptability	Low	High
Building time	Low	High
Building complexity	Low	High
Main advantage	Relatively quick solution	Future improvements
Use case	'One time only'	Multiple future use cases

3.2.2. Geometries of wheel and rail

In Figures A.1-A.5 of Appendix A the geometries of both rail and wheel(set) can be found. For the rail, the standardised 54E1 profile is used since it is most used in the Dutch railway network. The wheel(set) geometry is from the Dutch InterCityMaterieel (ICM) carriage with a S1002 wheel tread profile. The ICM train can be seen in Figure 3.2. The first carriages went in 1977 into service, at time of writing this carriage is still used daily for passenger transport on the domestic and Dutch high speed (180 km/h) railway network. Since it was never design for high speed, it is an interesting case to use in the model but is not researched.

Figure 3.2: Dutch ICM train (picture from Railway Engineering, TU Delft)

3.2.3. Preprocessing

In the preprocessing phase the geometry is build first. The global and local coordinate systems for the wheel and rail are defined. Which parameters, these systems can be translated or rotated to change the relative position of the wheel and rail. A 2D-line model is created from manual defined 2D keypoints (Figure 3.3) based on the cross sectional line geometries of the wheel and rail as seen in Appendix A. From this 2D-line geometries cross sectional area geometries are created(Figure 3.4). Here, the cross sectional mesh is defined (Figure 3.5). In the contact area (wheel tread and rail head) the mesh size is defined through a predefined parameter. The areas are transformed into volumes by rotating and extruding the area geometries of the wheel around its axis and rail in longitudinal direction respectively. Simultaneously all 4-node hexagonal area mesh elements are transformed into 3D solid elements (8-node brick) with respect to the geometry volumes(Figures 3.6 and (Figure 3.7). Dimensions of the elements are set by a parameter.

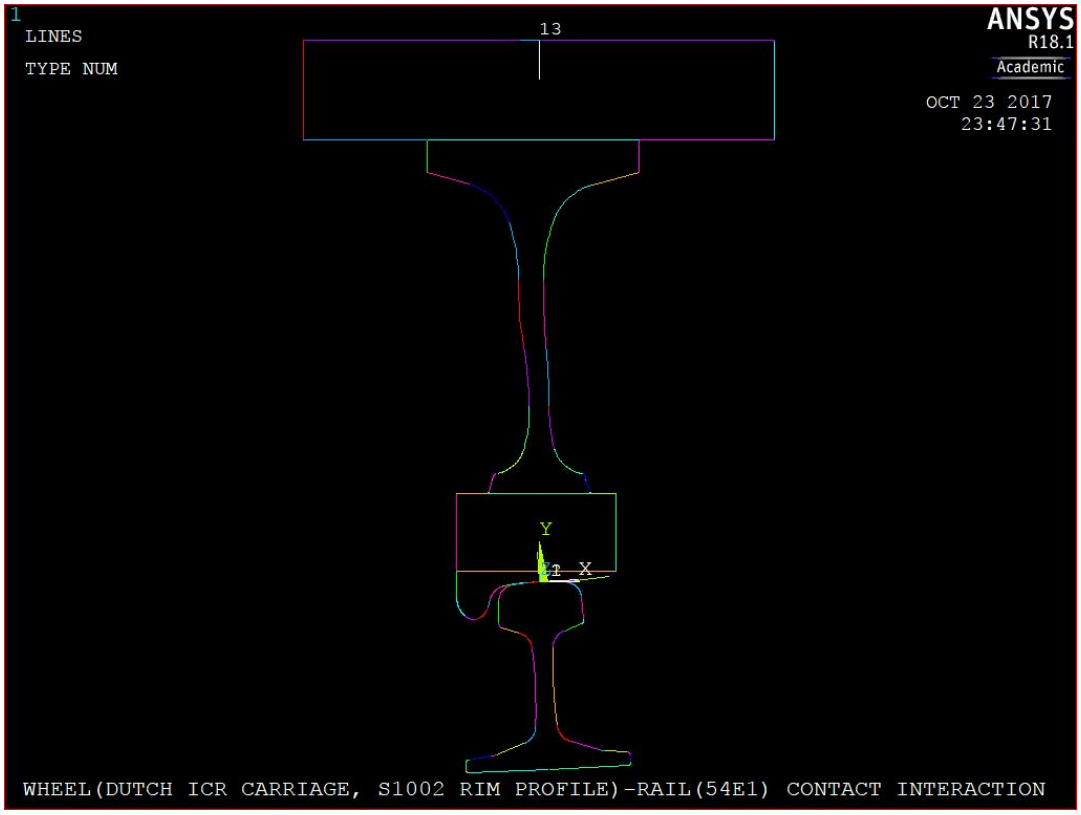

Figure 3.3: 2D line model

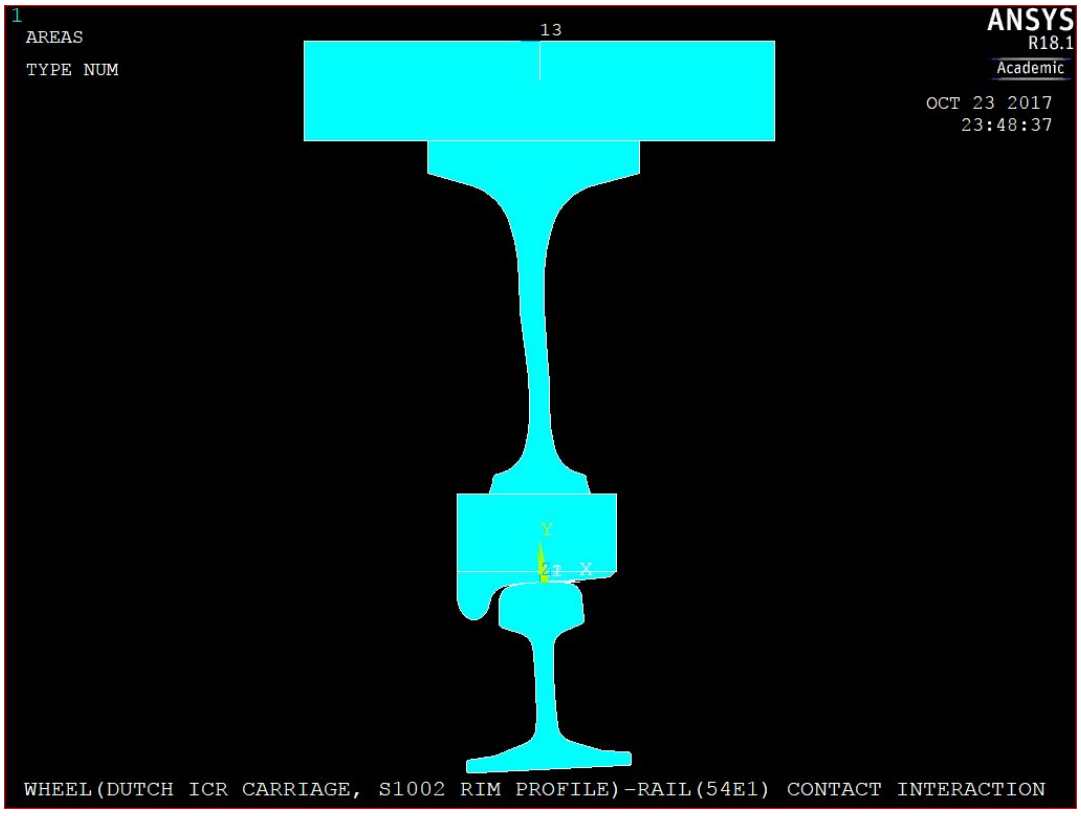

Figure 3.4: 2D area model

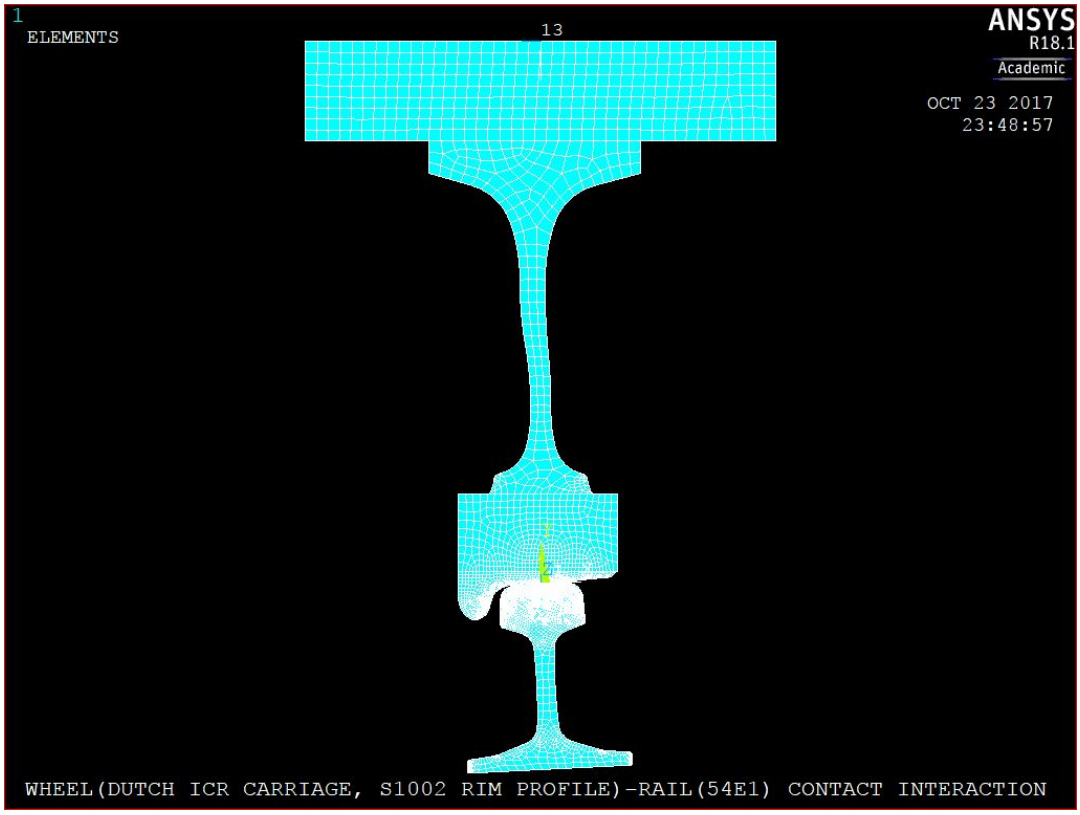

Figure 3.5: Meshed 2D area model

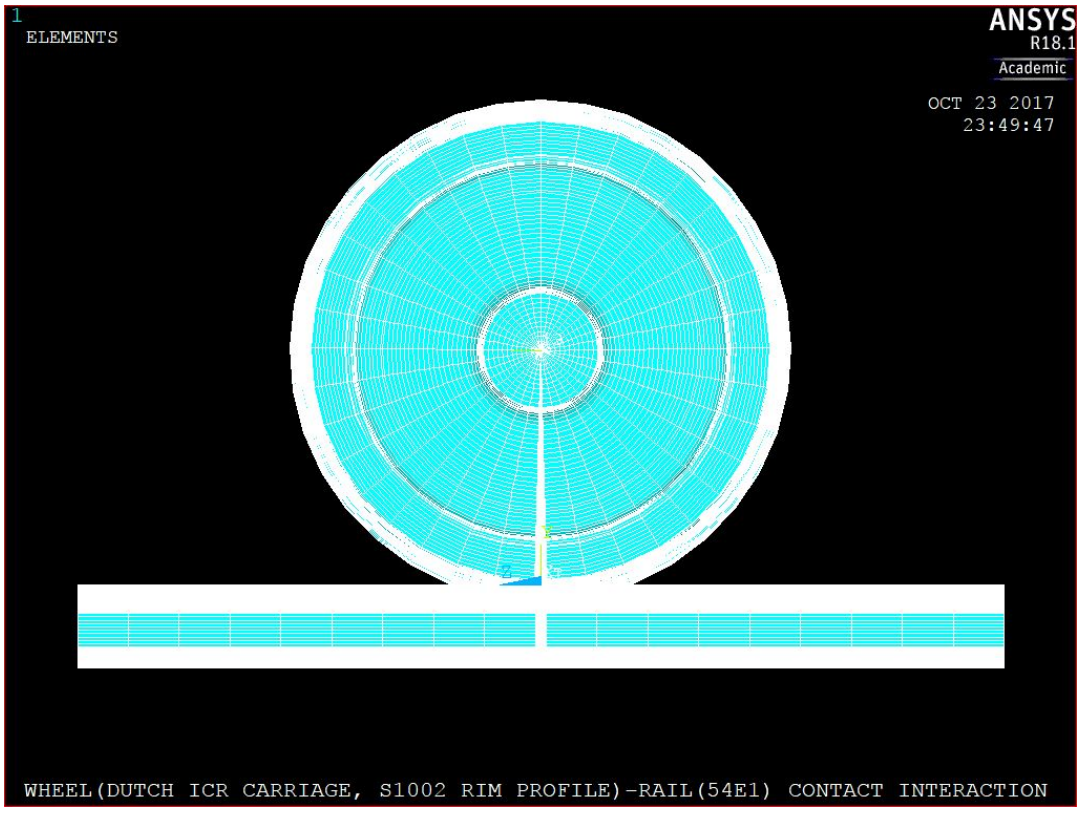

Figure 3.6: Meshed 3D element model

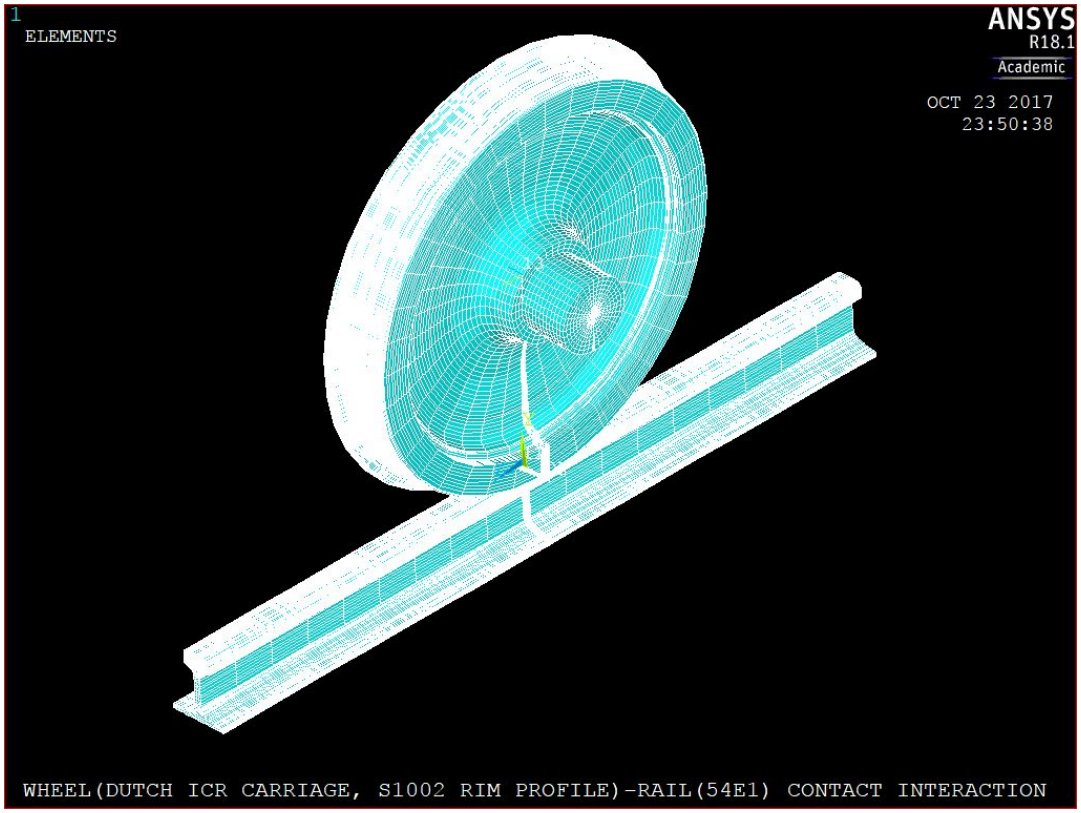

Figure 3.7: Meshed 3D element model

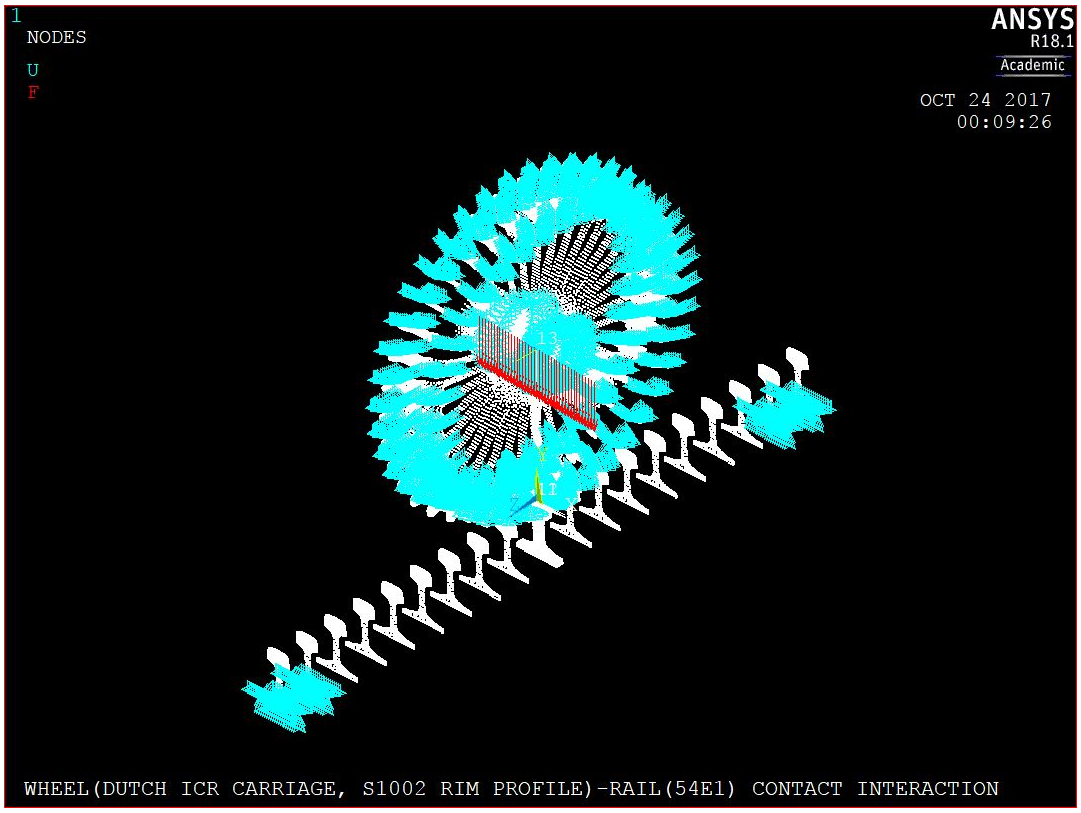

Figure 3.8: Distributed force and boundary conditions

At this point, the geometry is defined and is discretised into nodes and elements. A linear elastic isotropic material model is used to model the behaviour of steel. The arguments used are the Young's modulus and Poission's ratio. A parametric predefined total force is applied to the axle by determining the number of nodes in the centreline of the axle, to every node a even fraction of the total load is applied. At the bottom of the rail at each end, the rail is fixed by defining zero displacement. This fixing is dimensionally equal to the width of a sleeper with real inter-sleeper distance of 60 cm. The outer nodes of the wheel are constrained by only having a degree of freedom in vertical direction with respect to the rail (Figure 3.8).

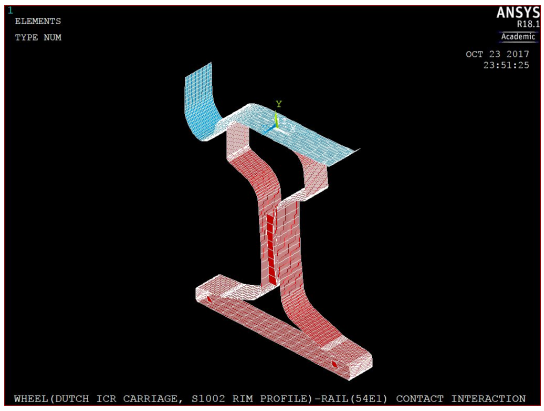

Figure 3.9: Contact pair

The model is now fully defined, except for the contact. This is defined by so called contact pairs. In a pair-based contact definition (Figure 3.9), the 3D contact surface elements (on the wheel) are associated with 3D target segment elements (on the rail). The program looks for contact interaction only between surfaces with the same real constant set ID (which is greater than zero). There are many element types that can be used for modelling contact. The element type used in this model determines contact stress by defining a linear spring in between two penetration elements.

So, the features of this model are:

- Automatic self-building with respect to predefined parameters
- Realistic geometry according to norms and technical drawings
- Individual coordinate systems and thus easy relative positioning of wheel and rail

The following parameters are automatically processed:

- Axle length
- Applied load (distributed evenly along axle nodes)
- Number of wheel segments for reducing (computational time)
- Element size inside and outside of the wheel contact volume
- Rail length
- Inter sleeper distance
- Sleeper width (for fixed boundary condition)
- Element size inside and outside of the rail contact volume

Now the whole model is defined and ready to be numerically solved. The sparse solver is used, and it takes about 10 minutes to solve completely. The values for all parameters can be found in the beginning of Appendix B.

3.2.4. Postprocessing

The FEM solution can be seen in Figures 3.10 and 3.11. The maximum pressure can be found in the middle of the contact patch, as expected. The contact patch has an elliptical shape, with a consistent pressure distribution. In the following chapter, the contact patch will be further analysed.

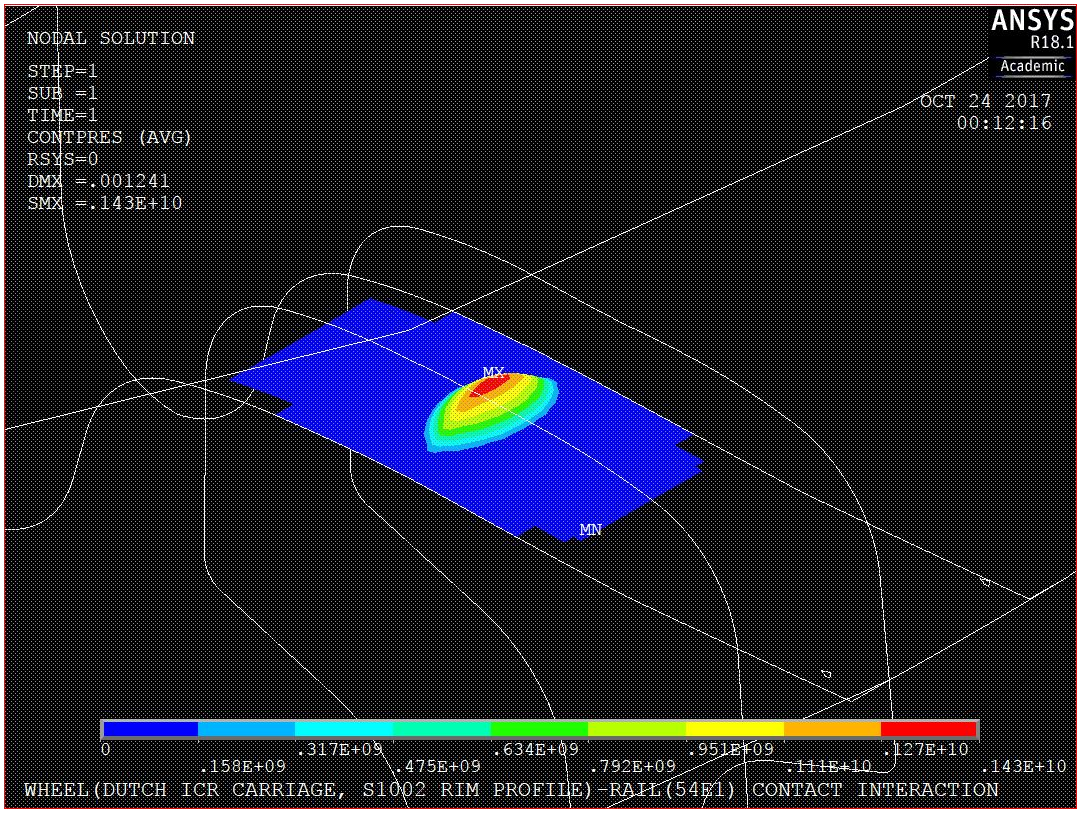

Figure 3.10: 3D contact pressure distribution

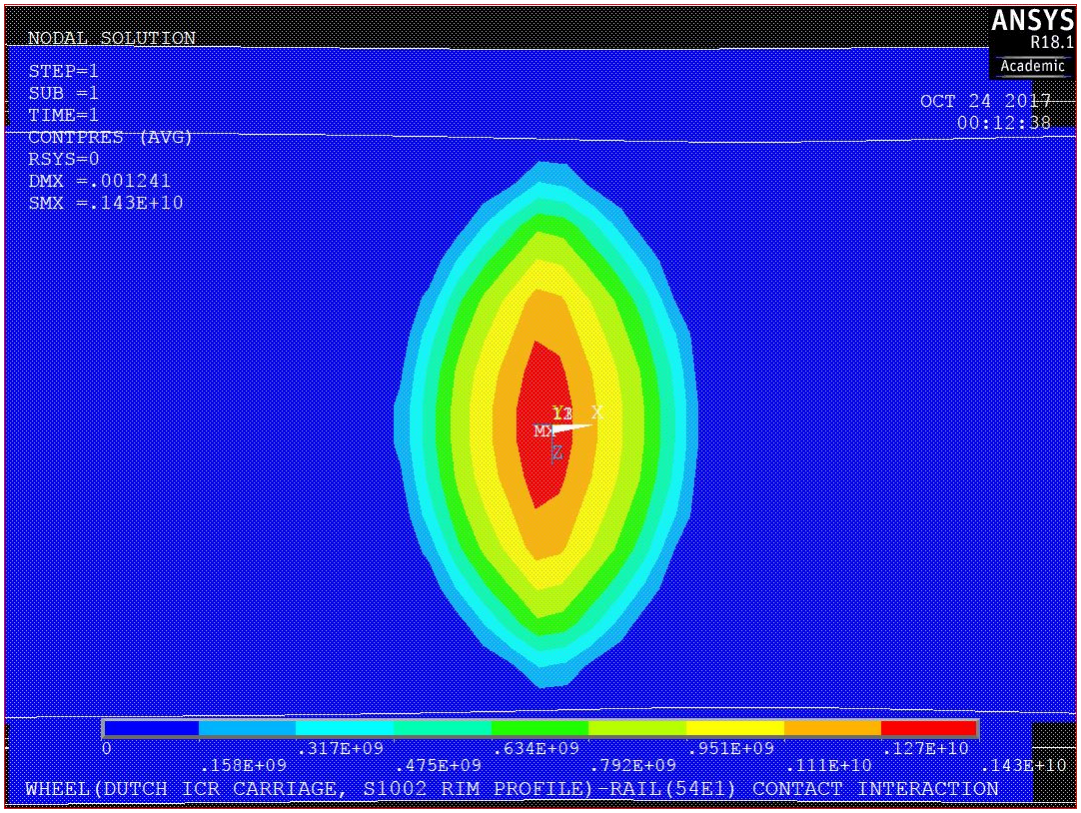

Figure 3.11: 2D contact pressure distribution

3.3. Validation of FE-model

3.3.1. Importance of validation

FEM has almost unlimited possibilities to solve physical problems. But with this freedom, solutions may vary and thus validation of the solution is of utmost importance. Often, experimental data (from measurements for instance) is used as a reference to the FE solution. When this is not available, theoretical or analytical solutions can be used for the same purpose. As said before, Heinrich Hertz (and many others) have developed contact theories. Since the aim of this paper is not to teach fundamental contact mechanics, only the basics is covered and proof of theories and formulas can be found in the references mentioned.

3.3.2. Analytical solution to wheel-rail contact

The specific geometry used in the contact problem described in this paper can be found in Appendix A. In Figure A.3 the diameter of the wheel can be found to be 960 mm, thus $R_1 = 460$ mm. From Figure A.1 can be concluded that the principal transverse radius is ∞ since the tread is assumed to be perfectly straight, thus $R_1' = \infty$. In Figure A.5 can be seen that $R_2' = 300$ mm (transversal direction perpendicular to principal radius of the wheel). Since we assume the rail to be perfectly straight in the principal transverse (longitudinal) direction, $R_2 = \infty$. The rail has an inclination of 1/20 relative to the wheel, thus the normal contacting planes are parallel to each other ($\phi = 0°$). As a material, for both the wheel and rail steel is used where $E_W = E_R = 210$ GPa and $\sigma_W = \sigma_R = 0.3$. The wheel load is half of the maximum allowed axle load of loading class D4 (22.5 tonne) which is most used in the Netherlands, thus $P = 112.5$ kN. So, the analytical problem variables are

$$\begin{cases} R_1 = 0.460 \text{ m} \\ R_1' = \infty \\ R_2 = \infty \\ R_2' = 0.300 \text{ m} \\ \phi = 0° \\ E_W = E_R = 210 \cdot 10^9 \text{ N/m}^2 \\ \sigma_W = \sigma_R = 0.3 \\ P = 112{,}500 \text{ N}. \end{cases} \tag{3.1}$$

Substitution of (3.1) in (2.9), (2.11) and (2.14) leads to

$$K_1 = K_2 = \frac{1 - 0.3^2}{\pi \cdot 210 \cdot 10^9} \approx 1.379 \cdot 10^{-12}, \tag{3.2}$$

$$K_3 = \frac{1}{2}\left(\frac{1}{0.460} + \frac{1}{\infty} + \frac{1}{\infty} + \frac{1}{0.300}\right) = \frac{1}{2}\left(\frac{1}{0.460} + \frac{1}{0.300}\right) \approx 2.754, \tag{3.3}$$

$$\begin{aligned} K_4 &= \frac{1}{2}\left[\left(\frac{1}{0.460} - \frac{1}{\infty}\right)^2 + \left(\frac{1}{\infty} - \frac{1}{0.300}\right)^2 + 2\left(\frac{1}{0.460} - \frac{1}{\infty}\right)\left(\frac{1}{\infty} - \frac{1}{0.300}\right)\cos(2 \cdot 0)\right] \\ &= \frac{1}{2}\left[\left(\frac{1}{0.460}\right)^2 + \left(-\frac{1}{0.300}\right)^2 + 2\left(\frac{1}{0.460}\right)\left(-\frac{1}{0.300}\right)\right] \\ &\approx 0.672. \end{aligned} \tag{3.4}$$

Substituting obtained values of K_3 and K_4 into (2.12) results in

$$\theta = \cos^{-1}\left(\frac{0.672}{2.754}\right) \approx 1.324 \text{ rad} \approx 75.872°. \tag{3.5}$$

Now, from Figure 2.5 the values for m and n can be obtained for determining a and b. Since θ is not exactly one of the values mentioned in the table, linear interpolation is used to derive m and n for non-tabled values of θ and thus errors in the analytical solution are introduced here. Besides, the values in the table already contain errors since the are numerically derived [3] and therefore are already an approximation. Nevertheless these values will be used for validation purposes to the FEM solution, but please note that the analytical solution possibly contains errors.

As said before, linear interpolation is used for obtaining values of m and n. $75° \leq \theta \leq 80°$ yields

$$\begin{aligned} m &= m_{75^\circ} + (\theta - 75^\circ) \cdot \frac{m_{80^\circ} - m_{75^\circ}}{80^\circ - 75^\circ}, \\ n &= n_{75^\circ} + (\theta - 75^\circ) \cdot \frac{n_{80^\circ} - n_{75^\circ}}{80^\circ - 75^\circ} \end{aligned} \tag{3.6}$$

where

m_x is the value for m according to Figure 2.5,
n_x is the value for n according to Figure 2.5.

Substitution of $\theta = 75.87^\circ$ and the values according to Figure 2.5 into 3.6 yields

$$\begin{aligned} m &= 1.202 + (75.872^\circ - 75^\circ) \cdot \frac{1.128 - 1.284}{80^\circ - 75^\circ} \approx 1.189, \\ n &= 0.846 + (75.872^\circ - 75^\circ) \cdot \frac{0.893 - 0.893}{80^\circ - 75^\circ} \approx 0.854. \end{aligned} \tag{3.7}$$

Substitution of (3.1) to (3.3) and (3.7) into (2.7) and (2.8) results into a contact patch with semi-axes

$$a = 1.189[3\pi \cdot 112500 \cdot (2 \cdot 1.379 \cdot 10^{-12})/(4 \cdot 2.754)]^{1/3} \approx 7.64 \cdot 10^{-3} \text{ m}, \tag{3.8}$$

$$b = 0.854[3\pi \cdot 112500 \cdot (2 \cdot 1.379 \cdot 10^{-12})/(4 \cdot 2.754)]^{1/3} \approx 5.49 \cdot 10^{-3} \text{ m}, \tag{3.9}$$

Substitution into Equation 2.6 leads to a maximum contact pressure

$$p_0 = \frac{3 \cdot 112,500}{2\pi \cdot 7.64 \cdot 10^{-3} \cdot 5.49 \cdot 10^{-3}} \approx 1.28 \cdot 10^9 \text{ N/m}^2. \tag{3.10}$$

3.3.3. Comparison FEM and analytical solution

In Table 3.2 the absolute results and relative difference can be seen. The values from both solutions differ, which can have a number of reasons, for instance:

- The element size in the contact area is too big. This results in too rough interpolation between nodes and thus a less accurate solution,
- The element size outside the contact area is too big. This results in 'jumps' through the model and eventually influences the contact area,
- The contact element type is not representing real world contact behaviour,
- The analytical solution contains errors due to approximate (interpolated) values of m and n,
- The analytical solution is calculated based on a too simplified geometry and does not represent real wheel/rail contact behaviour.

Table 3.2: Analytical and FEM solution for a, b and p_0

Variable	Analytical	FEM	Difference (%)
a (m)	$7.64 \cdot 10^{-3}$	$8.24 \cdot 10^{-3}$	+7.81
b (m)	$5.49 \cdot 10^{-3}$	$5.39 \cdot 10^{-3}$	-1.83
p_0 (N/m^2)	$1.28 \cdot 10^9$	$1.43 \cdot 10^9$	+11.72

Since errors in the analytical solution are introduced due to numerical integration and linear interpolation to determine values of m and n, it is interesting to see what happens when the values of a and b of the FEM model are assumed to exactly be the analytical values. When substituting values of a and b from the FEM solution (as seen in Table 3.2) into Equation 2.6 we obtain the semi-analytical maximum contact pressure

$$p_0 = \frac{3 \cdot 112,500}{2\pi \cdot 8.24 \cdot 10^{-3} \cdot 5.39 \cdot 10^{-3}} \approx 1.21 \cdot 10^9 \text{ N/m}^2. \tag{3.11}$$

Table 3.3: analytical, semi-analytical and FEM maximum contact pressure

	p_0 (N/m^2)	Difference to analytical (%)	Difference to semi-analytical (%)
Analytical	$1.28 \cdot 10^9$	-	+8.79
Semi-analytical	$1.21 \cdot 10^9$	-5.47	-
FEM	$1.43 \cdot 10^9$	+11.72	+18.24

In Table 3.3 the differences in maximum pressure between the FEM model and (semi-)analytical solution can be seen. What is interesting, is that by assuming the semi-axes of the FEM solution are correct, the difference between the FEM and semi-analytical solution increases, suggesting the FEM solution is more accurate with respect to the fully analytical solution with comparable but slightly different contact patch and stress distribution. Since the maximum pressure is directly related to the contact patch dimensions, the difference in maximum stress can possibly be explained by researching when ether the real stress distribution is perfectly ellipsoidal as assumed before.

4

Conclusion and recommendations

Since the 1800's steam powered trains were running along tracks already without the wheel/rail contact problem ever been addressed. This was the case until Heinrich Hertz in 1881 was the first to mention it in one of his papers. He created the first theory about elastic bodies in contact, which found application in railway engineering very well.

The wheel-rail contact is source of many problems which can lead to serious damages, costs and can eventually cause severe accidents like derailments. Therefore, research related to this problem is necessary. The Finite Element Method can be used very well for modelling the wheel/rail contact problem. It is capable of handling complex geometries and accurate solving in a reasonable amount of time. The parametric modelling approach is very well suited for research since it is easy to expand or improved and changes can be made relatively easy. Nevertheless, further research needs to be done to conclude the proposed model is accurate.

I recommend to apply different loads and validated the FEM solution to the analytical solution. Several relative positions of wheel and rail need to be researched as well. If measurement data is available, validation with respect to measurements can be done to draw a secure conclusion about the accuracy of the model. Also different contact elements need to be explored for modelling contact behaviour fundamentally different.

A

Technical drawings of wheel and rail geometries

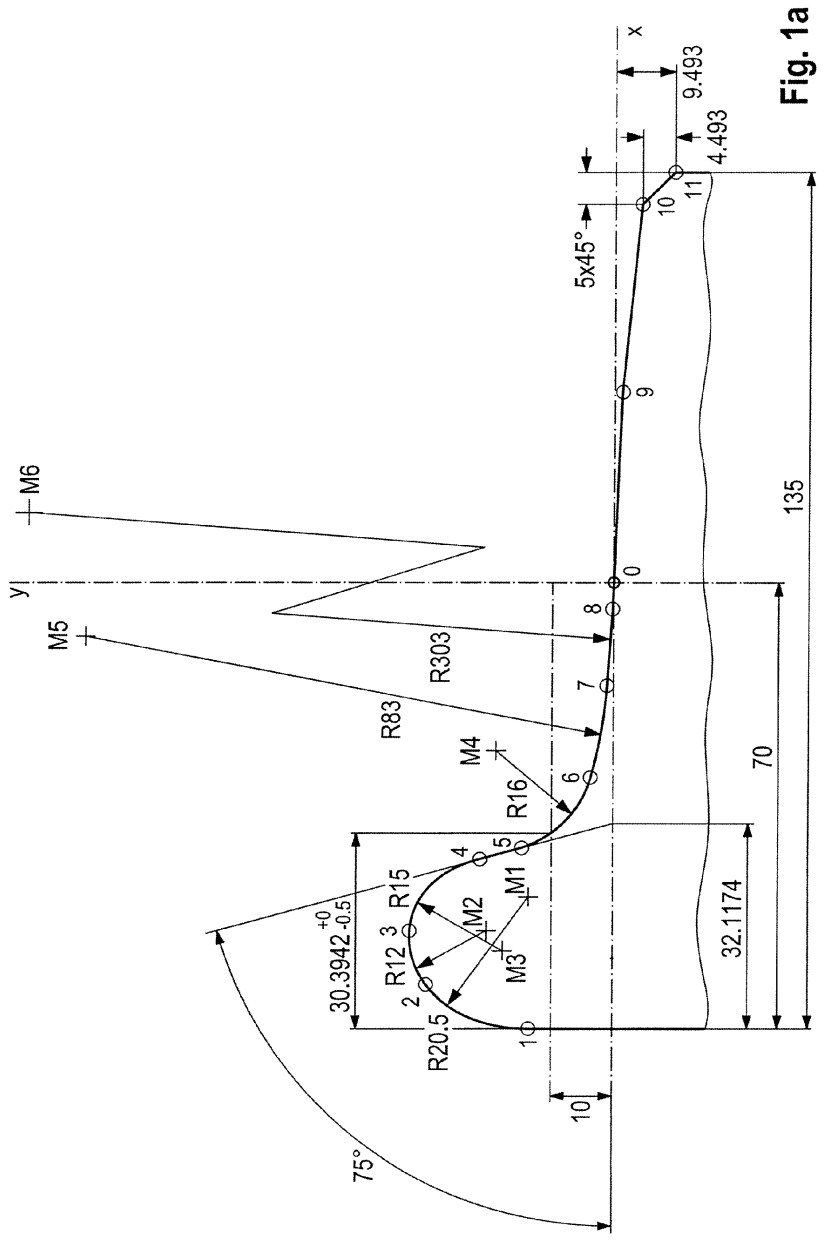

Figure A.1: Wheel tread geometry [6]

Pt.	X	Y	Pt.	X	Y	Pt.	X	Y
0	0.000	0.000	7	-16.208	1.046	M1	-49.5000	13.5910
1	-70.000	13.591	8	-4.255	0.212	M2	-55.0834	20.0000
2	-62.966	29.048	9	30.000	-1.499	M3	-58.0510	17.3140
3	-55.000	32.000	10	60.000	-4.493	M4	-26.4299	19.0772
4	-43.562	21.196	11	65.000	-9.493	M5	-8.7942	83.1745
5	-41.885	14.936				M6	10.8580	302.8350
6	-30.641	3.641						

Fig. 2a

3% Deviation

Pt.	X	Y		X_{max}	X_{min}		Delta X	Y_{max}	Y_{min}		Delta Y
1	-70.000	13.591		-67.900	-72.100		4.200	13.999	13.183		0.815
2	-62.966	29.048		-61.077	-64.855		3.778	29.919	28.177		1.743
3	-55.000	32.000		-53.350	-56.650		3.300	32.960	31.040		1.920
4	-43.562	21.196		-42.255	-44.869		2.614	21.832	20.560		1.272
5	-41.885	14.936		-40.628	-43.142		2.513	15.384	14.488		0.896
6	-30.641	3.641		-29.722	-31.560		1.838	3.750	3.532		0.218
7	-16.208	1.046		-15.722	-16.694		0.972	1.077	1.015		0.063
8	-4.255	0.212		-4.127	-4.383		0.255	0.218	0.206		0.013
9	30.000	-1.499		30.900	29.100		1.800	-1.454	-1.544		0.090
10	60.000	-4.493		61.800	58.200		3.600	-4.358	-4.628		0.270
11	65.000	-9.493		66.950	63.050		3.900	-9.208	-9.778		0.570

Fig. 2b

5% Deviation

Pt.	X	Y		X_{max}	X_{min}		Delta X	Y_{max}	Y_{min}		Delta Y
1	-70.000	13.591		-66.500	-73.500		7.000	14.271	12.911		1.359
2	-62.966	29.048		-59.818	-66.114		6.297	30.500	27.596		2.905
3	-55.000	32.000		-52.250	-57.750		5.500	33.600	30.400		3.200
4	-43.562	21.196		-41.384	-45.740		4.356	22.256	20.136		2.120
5	-41.885	14.936		-39.791	-43.979		4.189	15.683	14.189		1.494
6	-30.641	3.641		-29.109	-32.173		3.064	3.823	3.459		0.364
7	-16.208	1.046		-15.398	-17.018		1.621	1.098	0.994		0.105
8	-4.255	0.212		-4.042	-4.468		0.426	0.223	0.201		0.021
9	30.000	-1.499		31.500	28.500		3.000	-1.424	-1.574		0.150
10	60.000	-4.493		63.000	57.000		6.000	-4.268	-4.718		0.449
11	65.000	-9.493		68.250	61.750		6.500	-9.018	-9.968		0.949

Fig. 2c

Figure A.2: Wheel tread geometry coordinates [6]

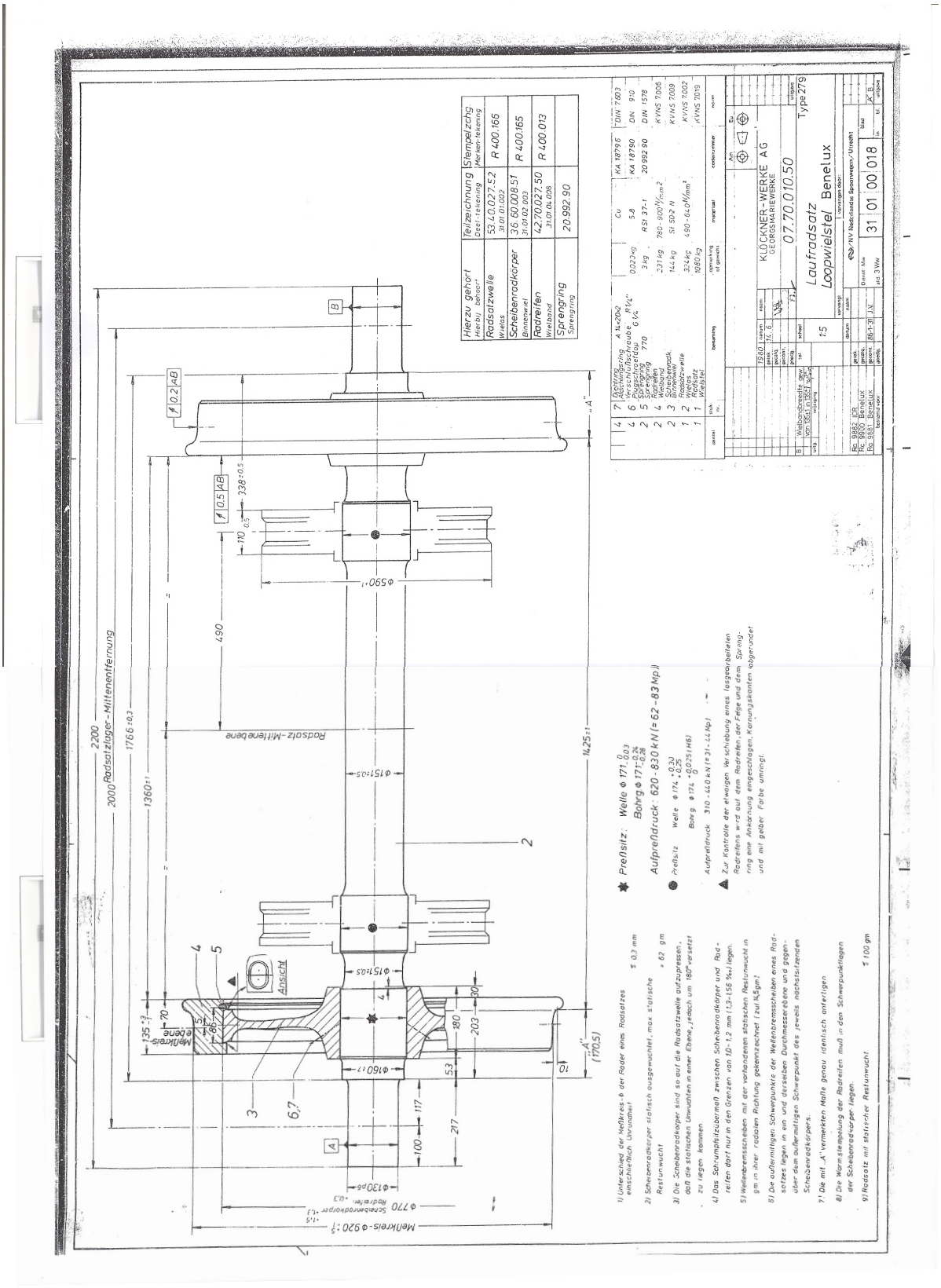

Figure A.3: Wheel set of Dutch carriage ICM

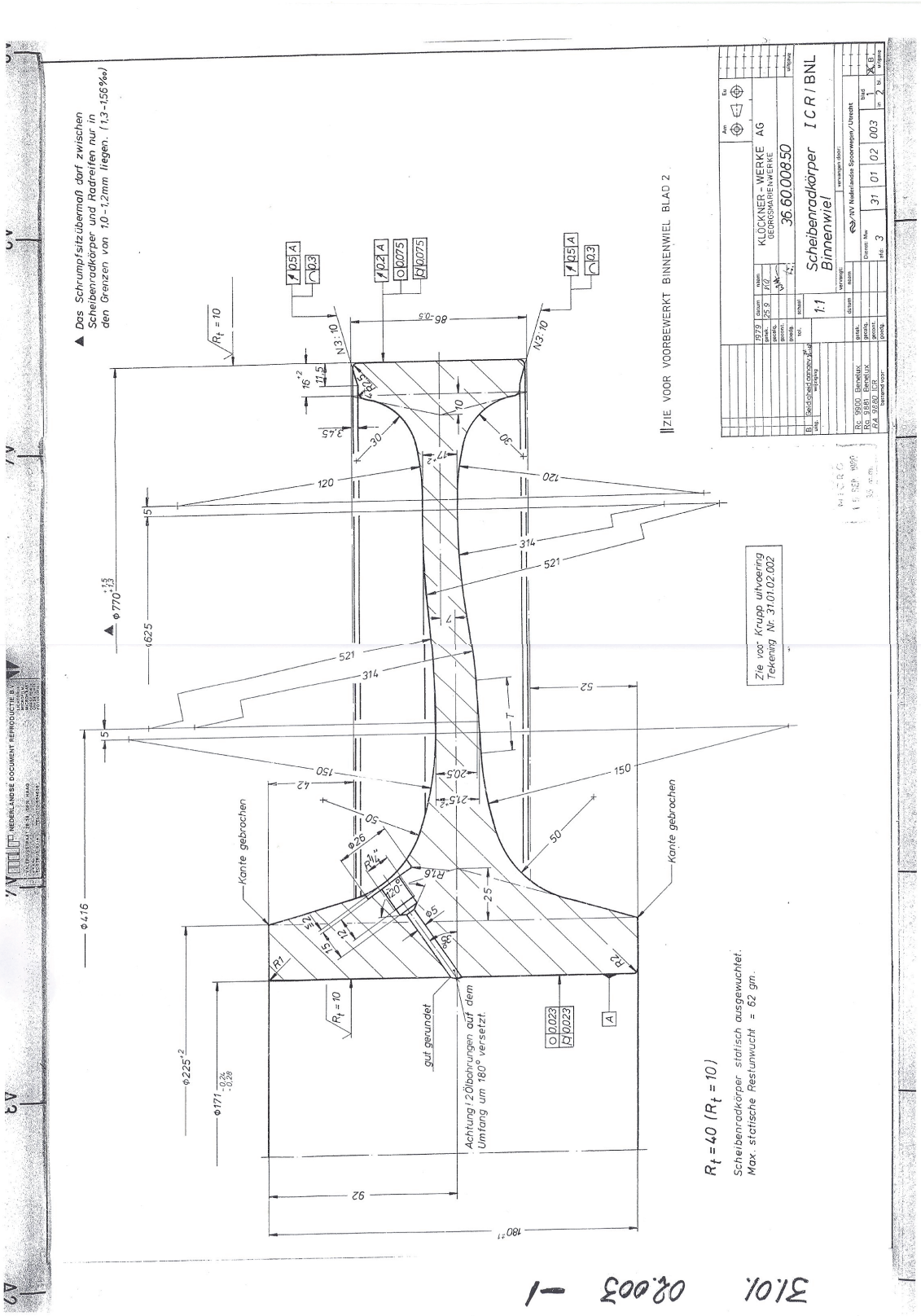
Das Schrumpfsitzübermaß darf zwischen Scheibenradkörper und Radreifen nur in den Grenzen von 1,0-1,2mm liegen. 1,3-1,56‰
ZIE VOOR VOORBEWERKT BINNENWIEL BLAD 2
Scheibenradkörper I C R / BNL
Binnenwiel
KLÖCKNER-WERKE AG
36.60.008.50
Zie voor Krupp uitvoering Tekening Nr. 31.01.02.002
Kante gebrochen
Kante gebrochen
gut gerundet
Achtung! Ölbohrungen auf dem Umfang um 180° versetzt.
Rt = 40 (Rt = 10)
Scheibenradkörper statisch ausgewuchtet.
Max. statische Restunwucht = 62 gm.
31.01 02.003 -1

Figure A.4

EN 13674-1:2011+A1:2017 (E)

Dimensions in millimetres

A1

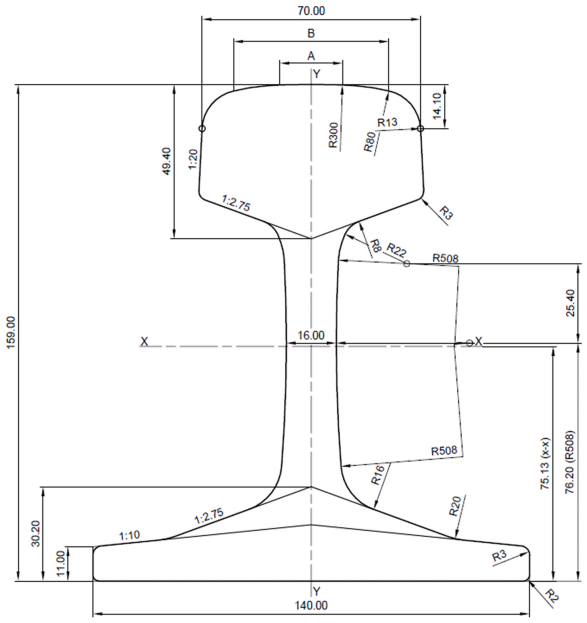

A1

Key

1 centre line of branding

cross-sectional area	:	69,77	cm^2
mass per metre	:	54,77	kg/m
moment of inertia x-x axis	:	2 337,9	cm^4
section modulus - Head	:	278,7	cm^3
section modulus - Base	:	311,2	cm^3
moment of inertia y-y axis	:	419,2	cm^4
section modulus y-y axis	:	59,9	cm^3
indicative dimensions:		*A* = 20,024 mm	
		B = 49,727 mm	

Figure A.15 — Rail profile 54E1

Figure A.5: Rail 54E1 (UIC54) geometry [1]

B

FEM model macro

```
! STATIC WHEEL-RAIL CONTACT MODEL !
! MODEL CREATED BY BOJAN BOGOJEVIC (B.BOGOJEVIC
    ↪ -2@STUDENT.TUDELFT.NL) !

/clear
/title, WHEEL(DUTCH ICR CARRIAGE, S1002 RIM
    ↪ PROFILE)-RAIL(54E1) CONTACT INTERACTION
/UNITS,SI
*AFUN,DEG

!!!!! GUI/OPERATING PARAMETERS !!!!!

! TOOLBAR BOXES FOR EXECUTING INDIVIDUAL
    ↪ SCRIPTS
*ABBR,TESTFILE,/INPUT,'TESTFILE','txt',,,
*ABBR,START,/INPUT,'START','txt',,,
*ABBR,WLINE,/INPUT,'W_LINE','txt',,,
*ABBR,RLINE,/INPUT,'R_LINE','txt',,,
*ABBR,WAREA,/INPUT,'W_AREA','txt',,,
*ABBR,RAREA,/INPUT,'R_AREA','txt',,,
*ABBR,WVOLUME,/INPUT,'W_VOLUME','txt',,,
*ABBR,RVOLUME,/INPUT,'R_VOLUME','txt',,,
*ABBR,WMESH,/INPUT,'W_MESH','txt',,,
*ABBR,RMESH,/INPUT,'R_MESH','txt',,,
*ABBR,FORCE,/INPUT,'FORCE','txt',,,
*ABBR,BC,/INPUT,'BC','txt',,,
*ABBR,CONTACT,/INPUT,'CONTACT','txt',,,
*ABBR,START_SOLVE,/INPUT,'START_SOLVE','txt',,,
*ABBR,POST,/INPUT,'POST','txt',,,
*ABBR,POSTANALYSIS,/INPUT,'POSTANALYSIS','txt',,,
*ABBR,PLOTSAVE,/INPUT,'PLOTSAVE','txt',,,
*ABBR,MULTIPLOT,/INPUT,'MULTIPLOT','txt',,,



! SCRIPTS AUTORUN SETTINGS (0=OFF,1=ON)
*SET,AUTORUN_W_LINE ,0
*SET,AUTORUN_W_AREA ,0
*SET,AUTORUN_W_VOLUME ,0
*SET,AUTORUN_W_MESH ,0
*SET,AUTORUN_R_LINE ,0
*SET,AUTORUN_R_AREA ,0
*SET,AUTORUN_R_VOLUME ,0
*SET,AUTORUN_R_MESH ,0

*SET,AUTORUN_W_MESH_SWEEP,1

! NUMBERING VIEW OPTIONS
*SET,V_N_KP ,0
*SET,V_N_LINE ,0
*SET,V_N_AREA ,0
*SET,V_N_VOLUME,0
/VIEW,1,1,1,1




!!!!! GLOBAL MODEL PARAMETERS !!!!!

! MATERIAL PARAMETERS
*SET,EXX,2.1E11
*SET,PR_XY,.3

! DEFINING MATERIAL PROPERTIES (ISOTROPIC, LINEAR
    ↪ MATERIAL, ONLY YOUNG'S MODULUS AND
    ↪ POISSON RATIO DEFINED)
/PREP7
MPTEMP,,,,,,,,
MP,EX,1,EXX
MP,PRXY,1,PR_XY

! DEFINING ELEMENT TYPES
ET,1,200,6
ET,2,185,,3




!!!!! GEOMETRY PARAMETERS !!!!!

! PARAMETERS WHEEL
*SET,W_F   ,112.5E3 ! TOTAL APPLIED FORCE, UNIFORM
    ↪ DISTRIBUTED OVER AXLE LENGTH
*SET,W_D   ,0.92 ! OUTER WHEEL DIAMETER (
```

```
      ↪ EXCLUDING FLANGE)
*SET,W_AXLE_D ,0.17 ! AXLE DIAMETER
*SET,W_ROT_GYRA ,360 ! WHEEL GYRADIUS
*SET,W_ROT_SEG ,18 ! # OF AXIAL WHEEL SEGMENTS
      ↪ FOR HALF WHEEL (TOTAL AXIALE SEGMENTS
      ↪ WILL BE *2)
*SET,W_AXLE_L ,0.4 !
*SET,W_CONTACT_DEGREE,3
*SET,W_CONTACT_ELEMLENGTH,1/1000
*SET,W_CONTACT_ELEMWIDTH,1/1000


! LOCAL COORDINATE SYSTEM WHEEL (#11)

*SET,W_P_DELTAX,0
*SET,W_P_DELTAY,0
*SET,W_P_DELTAZ,0
*SET,W_P_THETAX,0
*SET,W_P_THETAY,0
*SET,W_P_THETAZ,0

LOCAL,11,0,W_P_DELTAX,W_P_DELTAY,W_P_DELTAZ,
      ↪ W_P_THETAX,W_P_THETAY,W_P_THETAZ,,
CLOCAL,13,1,,W_D/2,,270,90,0 ! DEFINED RELATIVE TO
      ↪ CARTHESIAN LOCAL COORDINATE SYSTEM




! PARAMETERS RAIL
*SET,R_L,0.9
*SET,R_SLEEPER_DIST,0.6
*SET,R_SLEEPER_WIDTH,0.3
*SET,R_CONTACT_TARGETLENGTH,20/1000
*SET,R_CONTACT_ELEMLENGTH,1/1000
*SET,R_CONTACT_ELEMWIDTH,1/1000
*SET,R_ELEMLENGTH,100/1000


! LOCAL COORDINATE SYSTEM RAIL (#12)

*SET,R_P_DELTAX,0
*SET,R_P_DELTAY,0
*SET,R_P_DELTAZ,0
*SET,R_P_THETAX,1/20*360/(2*3.14159265359)
*SET,R_P_THETAY,0
*SET,R_P_THETAZ,0

LOCAL,12,0,R_P_DELTAX,R_P_DELTAY,R_P_DELTAZ,
      ↪ R_P_THETAX,R_P_THETAY,R_P_THETAZ,,




!!!!! AUTORUN EXECUTION !!!!!

*IF,AUTORUN_W_LINE,EQ,1,THEN
/INPUT,'W_LINE','txt',,,
/WAIT,.5
*ENDIF

*IF,AUTORUN_W_AREA,EQ,1,THEN
/INPUT,'W_AREA','txt',,,
/WAIT,.5
*ENDIF

*IF,AUTORUN_W_VOLUME,EQ,1,THEN
/INPUT,'W_VOLUME','txt',,,
/WAIT,.5
*ENDIF

*IF,AUTORUN_W_MESH,EQ,1,THEN
/INPUT,'W_MESH','txt',,,
/WAIT,.5
*ENDIF




*IF,AUTORUN_R_LINE,EQ,1,THEN
/INPUT,'R_LINE','txt',,,
/WAIT,.5
*ENDIF

*IF,AUTORUN_R_AREA,EQ,1,THEN
/INPUT,'R_AREA','txt',,,
/WAIT,.5
*ENDIF

*IF,AUTORUN_R_VOLUME,EQ,1,THEN
/INPUT,'R_VOLUME','txt',,,
/WAIT,.5
*ENDIF

*IF,AUTORUN_R_MESH,EQ,1,THEN
/INPUT,'R_MESH','txt',,,
/WAIT,.5
*ENDIF



!!!!!!!!!!!!!!!!!!!!!!!!!!!!!!!!!!!!!!!!!!!!!!!!!!!!!!!!!!!!!!!!!!!!!!!!!!!!!!!
/PREP7
CSYS,11
NUMSTR,KP,1
NUMSTR,LINE,1
NUMSTR,AREA,1
NUMSTR,VOLUME,1

!CLOCAL,14,0,,,,,-W_CONTACT_DEGREE/2 !ROTATION
      ↪ FOR FINE MESH VOLUME
!CSYS,14

! TREAD KEYPOINTS

K,0,0,0,0,
K,1,-70/1000,13.591/1000,0,
K,2,-62.966/1000,29.048/1000,0,
K,4,-43.562/1000,21.196/1000,0,
K,3,-55/1000,32/1000,0,
```

```
K,5,−41.885/1000,14.936/1000,0,
K,6,−30.641/1000,3.641/1000,0,
K,7,−16.208/1000,1.046/1000,0,
K,8,−4.255/1000,0.212/1000,0,
K,9,30/1000,−1.499/1000,0,
K,10,60/1000,−4.493/1000,0,
K,11,65/1000,−9.493/1000,0,
K,12,65/1000,−75/1000,0
K,13,W_AXLE_L/2,−(W_D/2)+(W_AXLE_D/2),0
K,14,W_AXLE_L/2,−(W_D/2),0
K,15,−W_AXLE_L/2,−(W_D/2),0
K,16,−W_AXLE_L/2,−(W_D/2)+(W_AXLE_D/2),0
K,17,−70/1000,−75/1000,0
K,18,−70/1000,−9.493/1000,0,

K,21,43/1000,−75/1000,0
K,22,(43−3.45)/1000,−(11.5+75)/1000,0
K,23,(43−3.45)/1000,−(16+75)/1000,0
K,24,0.189E−01,−0.962E−01,0
K,26,17/2/1000,−145/1000,0
K,27,17/2/1000,−150/1000,0
K,28,0.582E−02,−200/1000,0

K,30,3.75/1000,−257/1000,0
K,31,0.231E−01,−0.331,0
K,34,85/1000,−347.5/1000,0
K,35,85/1000,−375/1000,0




K,41,−43/1000,−75/1000,0
K,42,−(43−3.45)/1000,−(11.5+75)/1000,0
K,43,−(43−3.45)/1000,−(16+75)/1000,0
K,44,−0.189E−01,−0.962E−01,0
K,46,−17/2/1000,−145/1000,0
K,47,−17/2/1000,−150/1000,0
K,48,−0.129E−01,−200/1000,0

K,50,−17.75/1000,−257/1000,0
K,51,−0.373E−01 ,−0.331,0
K,54,−95/1000,−347.5/1000,0
K,55,−95/1000,−375/1000,0


! ARC CENTERPOINTS

K,71,(120+17/2)/1000,−142.5/1000,0
K,72,−(521−17/2)/1000,−147.5/1000,0
K,73,(521+20.497/2−7)/1000,−252/1000 !! NO
    ↪ INTERSECTION WHEN WEB WIDTH = 20.5MM
    ↪ AS IN THE DRAWINGS
K,74,(21.5/2+150−7)/1000,−257/1000

K,81,−(120+17/2)/1000,−142.5/1000,0
K,82,−(314+17/2)/1000,−147.5/1000,0
K,83,(314+20.507/2−7)/1000,−252/1000 !! NO
    ↪ INTERSECTION WHEN WEB WIDTH = 20.5MM
    ↪ AS IN THE DRAWINGS
K,84,−(21.5/2+150+7)/1000,−257/1000

K,91,−49.5/1000,13.5910/1000,0,
K,92,−55.0834/1000,20/1000,0,
K,93,−58.0510/1000,17.314/1000,0,
K,94,−26.43/1000,19.0772/1000,0,
K,95,−8.7942/1000,83.1745/1000,0,
K,96,10.858/1000,302.835/1000,0,


! TREAD LINES

LARC,1,2,91,20.5/1000,
LARC,2,3,92,12/1000,
LARC,3,4,93,15/1000,
LSTR,4,5
LARC,5,6,94,16/1000,
LARC,6,7,95,83/1000,
LARC,7,8,96,303/1000,
LSTR,8,9
LSTR,9,10
LSTR,10,11


! WHEEL LINES

LSTR,11,12
!LSTR,12,13
LSTR,13,14
LSTR,14,15
LSTR,15,16
LSTR,16,55
LSTR,17,18
LSTR,18,1
LSTR,11,18

LSTR,13,35

NUMSTR,KP,20
NUMSTR,LINE,20

LSTR,12,21 !!!!!!!!

LSTR,21,22
LSTR,22,23
LSTR,23,24
LARC,24,26,71,120/1000,
LSTR,26,27
LARC,27,28,72,521/1000,
LARC,28,30,73,521/1000,
LARC,30,31,74,150/1000
LSTR,31,34
LSTR,34,35

LFILLT,20,21,2.5/1000,
LFILLT,22,23,4/1000,
LFILLT,23,24,30/1000,
LFILLT,28,29,50/1000,




NUMSTR,KP,40
NUMSTR,LINE,40
```

```
LSTR,17,41

LSTR,41,42
LSTR,42,43
LSTR,43,44
LARC,44,46,81,120/1000,
LSTR,46,47
LARC,47,48,82,314/1000,
LARC,48,50,83,314/1000,
LARC,50,51,84,150/1000

LSTR,51,54
LSTR,54,55

LFILLT,40,41,2.5/1000,
LFILLT,42,43,4/1000,
LFILLT,43,44,30/1000,
LFILLT,48,49,50/1000,

LSTR,20,40
LSTR,35,55


NUMMRG,KP,,,, ! MERGE COINCING KEY POINTS (DUE
    ↪ TO REFLECTING) FOR CONTINUITY
!LSYMM,X,1,99,,,,1
LSYMM,Y,1,99,,,,1

! CREATE LINE COMPONENTS

!! WHEEL TREAD
ALLSEL
LSEL,S,LINE,,1,99
LSEL,U,LINE,,11,16
LSEL,U,LINE,,19,99
CM,W_TREAD_LINE,LINE
CMSEL,NONE


!! WHEEL RIM

ALLSEL
LSEL,S,LINE,,11,55
LSEL,U,LINE,,12,15
LSEL,U,LINE,,17,17
LSEL,U,LINE,,19,19
LSEL,U,LINE,,21,39
LSEL,U,LINE,,41,54
CM,W_RIM_LINE,LINE
CMSEL,NONE


!! WHEEL WEB

ALLSEL
LSEL,S,LINE,,21,56
LSEL,U,LINE,,40,40
CM,W_WEB_LINE,LINE
CMSEL,NONE


!! WHEEL AXLE

ALLSEL
LSEL,S,LINE,,12,56
LSEL,U,LINE,,16,18
LSEL,U,LINE,,20,55
CM,W_AXLE_LINE,LINE
CMSEL,NONE

!! WHEEL ALL
CMSEL,NONE
ALLSEL
CMSEL,S,W_TREAD_LINE
CMSEL,A,W_RIM_LINE
CMSEL,A,W_WEB_LINE
CMSEL,A,W_AXLE_LINE
CM,W_ALL_LINE,LINE



! REFLECT KEYPOINTS AND LINES IN X−Z PLANE (
    ↪ GEOMETRY DEFINED UPSIDE DOWN)

!LSYMM,Y,W_TOTAL_LINE,,,,,1
!LSYMM,Y,W_TREAD_LINE,,,,,1
!LSYMM,Y,W_RIM_LINE,,,,,1
!LSYMM,Y,W_WEB_LINE,,,,,1
!LSYMM,Y,W_AXLE_LINE,,,,,1

CMSEL,NONE
CSYS,0
ALLSEL
*IF,V_N_KP,EQ,1,THEN
/PNUM,KP,1
*IF,V_N_LINE,EQ,1,THEN
/PNUM,LINE,1
LPLOT
!KPLOT

!!!!!!!!!!!!!!!!!!!!!!!!!!!!!!!!!!!!!!!!!!!!!!!!!!!!!!!!!!!!!!!!!!!!!!!!!!!!!!!
/PREP7
CSYS,12
NUMSTR,KP,100
NUMSTR,LINE,100
NUMSTR,AREA,100
NUMSTR,VOLUME,100

! LINE GEOMETRY RAIL
! HEAD KEYPOINTS
K,101,0,0,0
K,102,10.0/1000,−0.2/1000,0
K,103,24.9/1000,−2.0/1000,0
K,104,35/1000,−14.1/1000,0
K,105,36.1/1000,−36.3/1000,0
K,106,9.33/1000,−46.0/1000
K,107,0.1e−1,−133.0/1000
K,108,46.3/1000,−145.6/1000,0
K,109,70.0/1000,−148.0/1000,0
K,110,70.0/1000,−159.0/1000,0
```

```
K,111,0,−159/1000,0


! ARC CENTERPOINTS

K,191,0,−300/1000,0
K,192,7.3/1000,−80.1/1000,0
K,193,22.1/1000,−14.8/1000,0
K,194,516.0/1000,−82.8/1000,0


! LINES HEAD

NUMSTR,LINE,101
LARC,101,102,191,300/1000
LARC,102,103,192,80/1000
LARC,103,104,193,13/1000
LSTR,104,105
LSTR,105,106
LARC,106,107,194,508/1000
LSTR,107,108
LSTR,108,109
LSTR,109,110
LSTR,110,111

NUMSTR,KP,101
LFILLT,104,105,3/1000,
LFILLT,105,106,16/1000,
LFILLT,106,107,16/1000,
LFILLT,107,108,20/1000,
LFILLT,108,109,3/1000,
LFILLT,109,110,2/1000,

NUMSTR,KP,201
NUMSTR,LINE,201

LSYMM,X,100,200,,,,0

NUMMRG,KP,,,, ! MERGE COINCING KEY POINTS (DUE
    ↪ TO REFLECTING) FOR CONTINUITY

ALLSEL
LSEL,S,LINE,,100,200
LSEL,A,LINE,,200,300
CM,R_ALL_LINE,LINE

CMSEL,NONE
CSYS,0
ALLSEL
*IF,V_N_LINE,EQ,1,THEN
/PNUM,LINE,1
LPLOT
!!!!!!!!!!!!!!!!!!!!!!!!!!!!!!!!!!!!!!!!!!!!!!!!!!!!!!!!!!!!!!!!!!!!!!!!!!!!

/PREP7
CSYS,11
NUMSTR,KP,1
NUMSTR,LINE,1
NUMSTR,AREA,1
NUMSTR,VOLUME,1


! CREATE AREA COMPONENTS
!! WHEEL TREAD
CMSEL,NONE
LSEL,NONE
ASEL,NONE
CMSEL,S,W_TREAD_LINE
AL,W_TREAD_LINE
CM,W_TREAD_AREA,AREA



!! WHEEL RIM
CMSEL,NONE
CMSEL,S,W_RIM_LINE,LINE
AL,W_RIM_LINE

CM,W_RIM_AREA,AREA


!! WHEEL WEB
CMSEL,NONE
CMSEL,S,W_WEB_LINE
AL,W_WEB_LINE

CM,W_WEB_AREA,AREA


!! WHEEL AXLE
CMSEL,NONE
CMSEL,S,W_AXLE_LINE
AL,W_AXLE_LINE
CM,W_AXLE_AREA,AREA


!! TOTAL WHEEL AREA
CMSEL,NONE
ALLSEL
CMSEL,S,W_TREAD_AREA
CMSEL,A,W_RIM_AREA
CMSEL,A,W_WEB_AREA
CMSEL,A,W_AXLE_AREA
CM,W_ALL_AREA,AREA

!!!!!!!!!!!!!!!!!!!!!!!!!!!!!!!!!!!!!!!!!!!!!!!!!!!!!!!!!!!!!!!!!!!!!!!!!!!!

/PREP7
CSYS,12
NUMSTR,KP,100
NUMSTR,LINE,100
NUMSTR,AREA,100
NUMSTR,VOLUME,100

! CREATE AREA COMPONENTS
!! WEB

CMSEL,NONE
CMSEL,S,R_ALL_LINE,LINE

AL,R_ALL_LINE
ASLL,S
```

```
CM,R_ALL_AREA,AREA

CMSEL,NONE
CSYS,0
ALLSEL
*IF,V_N_AREA,EQ,1,THEN
/PNUM,AREA,1
APLOT




!!!!!!!!!!!!!!!!!!!!!!!!!!!!!!!!!!!!!!!!!!!!!!!!!!!!!!!!!!!!!!!!!!!!!!!!!!!!
CSYS,11

LSEL,S,LINE,,1,2
!LESIZE, NL1, SIZE, ANGSIZ, NDIV, SPACE, KFORC,
    ↪ LAYER1, LAYER2, KYNDIV
LESIZE,ALL,W_CONTACT_ELEMWIDTH*2,,,,,3,,1

LSEL,S,LINE,,3,9
!LESIZE, NL1, SIZE, ANGSIZ, NDIV, SPACE, KFORC,
    ↪ LAYER1, LAYER2, KYNDIV
LESIZE,ALL,W_CONTACT_ELEMWIDTH,,,,,5,,0

LSEL,S,LINE,,17,17
!LESIZE, NL1, SIZE, ANGSIZ, NDIV, SPACE, KFORC,
    ↪ LAYER1, LAYER2, KYNDIV
LESIZE,ALL,,,8,,,,,1

LSEL,S,LINE,,18,18
!LESIZE, NL1, SIZE, ANGSIZ, NDIV, SPACE, KFORC,
    ↪ LAYER1, LAYER2, KYNDIV
LESIZE,ALL,W_CONTACT_ELEMWIDTH*3,,,,,,,0

LSEL,S,LINE,,11,11
LSEL,A,LINE,,16,16
!LESIZE, NL1, SIZE, ANGSIZ, NDIV, SPACE, KFORC,
    ↪ LAYER1, LAYER2, KYNDIV
LESIZE,ALL,W_CONTACT_ELEMWIDTH*8,,,,,,,1

LSEL,S,LINE,,20,20
LSEL,A,LINE,,40,40
LESIZE,ALL,,,4,,,,,1

LSEL,A,LINE,,55,55
LESIZE,ALL,,,16,,,,,1



LSEL,S,LINE,,31,31
LSEL,A,LINE,,22,22
LSEL,A,LINE,,32,32
LSEL,A,LINE,,23,23
LSEL,A,LINE,,43,43
LSEL,A,LINE,,52,52
LSEL,A,LINE,,42,42
LSEL,A,LINE,,51,51
!LESIZE, NL1, SIZE, ANGSIZ, NDIV, SPACE, KFORC,
    ↪ LAYER1, LAYER2, KYNDIV
LESIZE,ALL,,,2,,,,,1

LSEL,S,LINE,,25,25
!LESIZE, NL1, SIZE, ANGSIZ, NDIV, SPACE, KFORC,
    ↪ LAYER1, LAYER2, KYNDIV
LESIZE,ALL,10/1000,,,,,,,1



LSEL,S,LINE,,W_WEB_LINE
LSEL,U,LINE,,31,31
LSEL,U,LINE,,22,22
LSEL,U,LINE,,32,32
LSEL,U,LINE,,23,23
LSEL,U,LINE,,43,43
LSEL,U,LINE,,52,52
LSEL,U,LINE,,42,42
LSEL,U,LINE,,51,51
LSEL,U,LINE,,56,56
LSEL,U,LINE,,25,25
!LESIZE, NL1, SIZE, ANGSIZ, NDIV, SPACE, KFORC,
    ↪ LAYER1, LAYER2, KYNDIV
LESIZE,ALL,10/1000,,,,,,,0

LSEL,S,LINE,,56,56
!LESIZE, NL1, SIZE, ANGSIZ, NDIV, SPACE, KFORC,
    ↪ LAYER1, LAYER2, KYNDIV
LESIZE,ALL,10/1000,,,,,1,3,0

LSEL,S,LINE,,15,15
LSEL,A,LINE,,19,19
!LESIZE, NL1, SIZE, ANGSIZ, NDIV, SPACE, KFORC,
    ↪ LAYER1, LAYER2, KYNDIV
LESIZE,ALL,10/1000,,,,,1,3,0

LSEL,S,LINE,,12,12
LSEL,A,LINE,,14,14
!LESIZE, NL1, SIZE, ANGSIZ, NDIV, SPACE, KFORC,
    ↪ LAYER1, LAYER2, KYNDIV
LESIZE,ALL,10/1000,,,,,,,0

LSEL,S,LINE,,13,13
!LESIZE, NL1, SIZE, ANGSIZ, NDIV, SPACE, KFORC,
    ↪ LAYER1, LAYER2, KYNDIV
LESIZE,ALL,10/1000,,,,,,,0



AMESH,W_TREAD_AREA
AMESH,W_RIM_AREA
AMESH,W_WEB_AREA
AMESH,W_AXLE_AREA

!!!!!!!!!!!!!!!!!!!!!!!!!!!!!!!!!!!!!!!!!!!!!!!!!!!!!!!!!!!!!!!!!!!!!!!!!!!!

/PREP7
CSYS,12

LSEL,S,LINE,,101,104
LSEL,A,LINE,,201,204
!LESIZE, NL1, SIZE, ANGSIZ, NDIV, SPACE, KFORC,
    ↪ LAYER1, LAYER2, KYNDIV
LESIZE,ALL,R_CONTACT_ELEMWIDTH,,,,,3,,1
```

```
CMSEL,S,R_ALL_LINE
!LESIZE, NL1, SIZE, ANGSIZ, NDIV, SPACE, KFORC,
    ↪ LAYER1, LAYER2, KYNDIV
LESIZE,ALL,,10,,,2,3,,1

CMSEL,S,R_ALL_LINE
!LESIZE, NL1, SIZE, ANGSIZ, NDIV, SPACE, KFORC,
    ↪ LAYER1, LAYER2, KYNDIV
LESIZE,ALL,,,10,,2,,,1

AMESH,R_ALL_AREA


!CMSEL,S,R_CONTACT_VOLUME,VOLUME
!ASLV,S
!LSLA,S
!LSEL,U,LOC,Z,-R_CONTACT_TARGETLENGTH/2,-
    ↪ R_CONTACT_TARGETLENGTH/2
!LSEL,U,LOC,Z,R_CONTACT_TARGETLENGTH/2,
    ↪ R_CONTACT_TARGETLENGTH/2
!LESIZE,ALL,R_CONTACT_ELEMLENGTH,,,,,,

!VSWEEP,R_CONTACT_VOLUME,R_ALL_AREA,
    ↪ R_CONTACT_TARGETAREAPOSITIVE
!VSWEEP,R_CONTACT_VOLUME,R_ALL_AREA,
    ↪ R_CONTACT_TARGETAREANEGATIVE




!CMSEL,S,R_ALL_VOLUME
!CMSEL,U,R_CONTACT_VOLUME
!ASLV,S,ALL
!LSLA,S,ALL
!LESIZE,ALL,R_ELEMLENGTH,,,,,,5,1
!VSWEEP,ALL,R_ALL_AREA

CMSEL,NONE
CSYS,0
ALLSEL
EPLOT

!!!!!!!!!!!!!!!!!!!!!!!!!!!!!!!!!!!!!!!!!!!!!!!!!!!!!!!!!!!!!!!!!!!!!!!!!!!!

/PREP7
CSYS,11
NUMSTR,KP,30000
NUMSTR,LINE,30000
NUMSTR,AREA,30000
NUMSTR,VOLUME,30000

ESIZE,,W_ROT_SEG

! CREATE VOLUMES
VROTAT,W_TREAD_AREA,,,,,,14,15,W_ROT_GYRA-
    ↪ W_CONTACT_DEGREE,2
VROTAT,W_RIM_AREA,,,,,,14,15,W_ROT_GYRA-
    ↪ W_CONTACT_DEGREE,2
VROTAT,W_WEB_AREA,,,,,,14,15,W_ROT_GYRA-
    ↪ W_CONTACT_DEGREE,2
VROTAT,W_AXLE_AREA,,,,,,14,15,W_ROT_GYRA-
    ↪ W_CONTACT_DEGREE,2

ESIZE,W_CONTACT_ELEMLENGTH

VROTAT,W_TREAD_AREA,,,,,,14,15,-
    ↪ W_CONTACT_DEGREE,1
VROTAT,W_RIM_AREA,,,,,,14,15,-W_CONTACT_DEGREE
    ↪ ,1
VROTAT,W_WEB_AREA,,,,,,14,15,-W_CONTACT_DEGREE
    ↪ ,1
VROTAT,W_AXLE_AREA,,,,,,14,15,-W_CONTACT_DEGREE
    ↪ ,1

CSYS,13
ALLSEL
VSEL,S,LOC,Y,360-W_CONTACT_DEGREE,360
CM,W_CONTACT_VOLUME,VOLUME
VSEL,R,LOC,X,,W_AXLE_D/2
CM,W_CONTACT_AXLE_VOLUME,VOLUME

ALLSEL
VSEL,S,LOC,Y,360-W_CONTACT_DEGREE,360
VSEL,R,LOC,X,,W_AXLE_D/2
CM,W_CONTACT_AXLE_VOLUME,VOLUME

ASLV,R
ASEL,R,LOC,Y,360-W_CONTACT_DEGREE/2+1,360-
    ↪ W_CONTACT_DEGREE/2-1
*GET,W_CONTACT_AXLE_TARGETAREA,AREA,0,NUM,
    ↪ MAX
APLOT


ALLSEL
VSEL,S,LOC,X,,W_D/2+9/1000
CM,W_ALL_VOLUME,VOLUME


ALLSELL
VGEN,,ALL,,,,W_CONTACT_DEGREE/2, , , ,1 !ROTATE
    ↪ WHEEL IN CORRECT POSITION
NUMMRG,ALL


ALLSEL

VSWEEP,W_ALL_VOLUME

ALLSEL
VSEL,S,LOC,Y,360-W_CONTACT_DEGREE,360
VSEL,R,LOC,X,,W_AXLE_D/2
CM,W_CONTACT_AXLE_VOLUME,VOLUME

ASLV,R
ASEL,R,LOC,Y,360-W_CONTACT_DEGREE/2+1,360-
    ↪ W_CONTACT_DEGREE/2-1
*GET,W_CONTACT_AXLE_TARGETAREA,AREA,0,NUM,
    ↪ MAX
APLOT
```

```
VSWEEP,W_CONTACT_AXLE_VOLUME,4,
    ↪ W_CONTACT_AXLE_TARGETAREA


CMSEL,S,W_CONTACT_VOLUME,VOLUME
VSEL,R,LOC,X,W_D/2-10/1000,W_D/2-10/1000+10
CM,W_CONTACT_TREAD_VOLUME,VOLUME

ALLSEL
EPLOT

!!!!!!!!!!!!!!!!!!!!!!!!!!!!!!!!!!!!!!!!!!!!!!!!!!!!!!!!!!!!!!!!!!!!!!!!

/PREP7
CSYS,12
NUMSTR,KP,20000
NUMSTR,LINE,20000
NUMSTR,AREA,20000
NUMSTR,VOLUME,20000

! CREATE VOLUMES
CMSEL,S,R_ALL_AREA,AREA
VEXT,R_ALL_AREA,,,,,R_CONTACT_TARGETLENGTH/2,1
VEXT,R_ALL_AREA,,,,,-R_CONTACT_TARGETLENGTH
    ↪ /2,1

VSEL,S,VOLU,,20000,21000
CM,R_CONTACT_VOLUME,VOLUME

CMSEL,S,R_CONTACT_VOLUME,VOLUME
ASLV,S
LSLA,S
LSEL,U,LOC,Z,-R_CONTACT_TARGETLENGTH/2,-
    ↪ R_CONTACT_TARGETLENGTH/2
LSEL,U,LOC,Z,R_CONTACT_TARGETLENGTH/2,
    ↪ R_CONTACT_TARGETLENGTH/2
LESIZE,ALL,R_CONTACT_ELEMLENGTH,,,,,,

VSWEEP,R_CONTACT_VOLUME,R_ALL_AREA,
    ↪ R_CONTACT_TARGETAREAPOSITIVE
VSWEEP,R_CONTACT_VOLUME,R_ALL_AREA,
    ↪ R_CONTACT_TARGETAREANEGATIVE

ASEL,S,LOC,Y,-10,0
ASEL,R,LOC,Z,-R_CONTACT_TARGETLENGTH
    ↪ /2-1/1000,-R_CONTACT_TARGETLENGTH/2
CM,R_CONTACT_TARTGETAREANEGATIVE,AREA
ESIZE,R_ELEMLENGTH
VEXT,ALL,,,,,-R_L,

ASEL,S,LOC,Y,-10,0
ASEL,R,LOC,Z,R_CONTACT_TARGETLENGTH/2,
    ↪ R_CONTACT_TARGETLENGTH/2+1/1000
CM,R_CONTACT_TARTGETAREAPOSITIVE,AREA
VEXT,ALL,,,,,R_L,



ALLSEL
VSEL,S,VOLU,,20000,21000
CM,R_ALL_VOLUME,VOLUME

CMSEL,S,R_ALL_VOLUME
CMSEL,U,R_CONTACT_VOLUME
ASLV,S,ALL
LSLA,S,ALL
LESIZE,ALL,R_ELEMLENGTH,,,,,,5,1
VSWEEP,ALL,R_ALL_AREA


CMSEL,NONE
CSYS,0
ALLSEL
*IF,V_N_VOLUME,EQ,1,THEN
/PNUM,VOLUME,1
VPLOT

!!!!!!!!!!!!!!!!!!!!!!!!!!!!!!!!!!!!!!!!!!!!!!!!!!!!!!!!!!!!!!!!!!!!!!!!

/PREP7
CSYS,13
! AXLE CENTER NODES COMPONENT

NSEL,S,LOC,X,0,1/1000
CM,W_LOAD_NODES,NODE
NPLOT

ALLSEL
CMSEL,NONE

! APPLY AXLE LOAD
CMSEL,S,W_LOAD_NODES,NODE
*GET,W_LOAD_NUMNODES,NODE,N,COUNT
F,W_LOAD_NODES,FY,-W_F/W_LOAD_NUMNODES

CMSEL,NONE
CSYS,11

!!!!!!!!!!!!!!!!!!!!!!!!!!!!!!!!!!!!!!!!!!!!!!!!!!!!!!!!!!!!!!!!!!!!!!!!

/PREP7

! RAIL BOUNDARY CONDITION

CSYS,12
NSEL,S,LOC,Z,-10,-(R_L-R_SLEEPER_WIDTH/2)
NSEL,A,LOC,Z,(R_L-R_SLEEPER_WIDTH/2),10
NSEL,R,LOC,Y,-158.5/1000,-160/1000
CM,R_BC_NODES,NODE
D,R_BC_NODES,ALL,0

! WHEEL BOUNDARY CONDITION
ALLSEL
CSYS,13
NSEL,S,LOC,Z,-66/1000,-64/1000
NSEL,A,LOC,Z,69/1000,70/1000
NSEL,R,LOC,X,W_D/2-(770/2/1000),W_D/2+10/1000
CM,W_BC_NODES,NODE
D,W_BC_NODES,UX,0
D,W_BC_NODES,UZ,0
```

```
CMSEL,NONE
ALLSEL
CSYS,11
/REPLOT

!!!!!!!!!!!!!!!!!!!!!!!!!!!!!!!!!!!!!!!!!!!!!!!!!!!!!!!!!!!!!!!!!!!!!!!!!!!!

/COM, CONTACT PAIR CREATION - START
CM,_NODECM,NODE
CM,_ELEMCM,ELEM
CM,_KPCM,KP
CM,_LINECM,LINE
CM,_AREACM,AREA
CM,_VOLUCM,VOLU
/GSAV,cwz,gsav,,temp
MP,MU,1,.5
MAT,1
MP,EMIS,1,7.88860905221e-031
R,3
REAL,3
ET,3,170
ET,4,174
R,3,,,5.0,0.1,0,
RMORE,,,1.0E20,0.0,1.0,
RMORE,0.0,0,1.0,,1.0,0.5
RMORE,0,1.0,1.0,0.0,,1.0
RMORE,,,,,,1.0
KEYOPT,4,4,0
KEYOPT,4,5,1
KEYOPT,4,7,0
KEYOPT,4,8,0
KEYOPT,4,9,0
KEYOPT,4,10,2
KEYOPT,4,11,0
KEYOPT,4,12,0
KEYOPT,4,2,0
KEYOPT,3,5,0


! Generate the target surface
CMSEL,S,R_CONTACT_VOLUME
ASLV,S



CM,_TARGET,AREA
TYPE,3
NSLA,S,1
ESLN,S,0
ESLL,U
ESEL,U,ENAME,,188,189
NSLE,A,CT2
ESURF
CMSEL,S,_ELEMCM
! Generate the contact surface
CMSEL,S,W_CONTACT_TREAD_VOLUME
ASLV,S

!SEL,S,,,1
!ASEL,A,,,30025
!ASEL,A,,,30126
!ASEL,A,,,30127
!ASEL,A,,,30128
!ASEL,A,,,30129
!ASEL,A,,,30130
!ASEL,A,,,30131
!ASEL,A,,,30132
!ASEL,A,,,30133
!ASEL,A,,,30134
!ASEL,A,,,30135
!ASEL,A,,,30136
!ASEL,A,,,30137
CM,_CONTACT,AREA
TYPE,4
NSLA,S,1
ESLN,S,0
NSLE,A,CT2 ! CZMESH patch (fsk qt-40109 8/2008)
ESURF
ALLSEL
ESEL,ALL
ESEL,S,TYPE,,3
ESEL,A,TYPE,,4
ESEL,R,REAL,,3
/PSYMB,ESYS,1
/PNUM,TYPE,1
/NUM,1
EPLOT
ESEL,ALL
ESEL,S,TYPE,,3
ESEL,A,TYPE,,4
ESEL,R,REAL,,3
CMSEL,A,_NODECM
CMDEL,_NODECM
CMSEL,A,_ELEMCM
CMDEL,_ELEMCM
CMSEL,S,_KPCM
CMDEL,_KPCM
CMSEL,S,_LINECM
CMDEL,_LINECM
CMSEL,S,_AREACM
CMDEL,_AREACM
CMSEL,S,_VOLUCM
CMDEL,_VOLUCM
/GRES,cwz,gsav
CMDEL,_TARGET
CMDEL,_CONTACT
/COM, CONTACT PAIR CREATION - END

!!!!!!!!!!!!!!!!!!!!!!!!!!!!!!!!!!!!!!!!!!!!!!!!!!!!!!!!!!!!!!!!!!!!!!!!!!!!

/SOLU
NSUBST,,10,1
LSWRITE
/STATUS,SOLU
SOLVE

!!!!!!!!!!!!!!!!!!!!!!!!!!!!!!!!!!!!!!!!!!!!!!!!!!!!!!!!!!!!!!!!!!!!!!!!!!!!
!END OF MACRO!
```

Bibliography

[1] Railway applications - track - rail - part 1: Vignole railway rails 46 kg/m and above, 2011.

[2] Vijay K. Garg and Rao V. Dukkipati. *Dynamics of Railway Vehicle Systems*. Academic Press Canada, 1984.

[3] J.A. Greenwood. *Formulas for moderately elliptical Hertzian contacts*. J. Tribology, 1885.

[4] Heinrich Hertz. *Miscellaneous papers*. Macmillan, 1896.

[5] D. A. Hills, D. Nowell, and A. Sackfield. *Mechanics of Elastic Contacts*. Butterworth-Heinemann Ltd, 1993.

[6] Wolfram Hoehne, Alfred Lohmann, Jani Dede, Mario Rettig, and Johannes Stephanides. Running profile of railway wheel, March 2010.

[7] David Hutton. *Fundamentals of Finite Element Analysis*. McGraw-Hill, 2004.

[8] K.L. Johnson. *Contact Mechanics*. Cambridge University Press, 1885.

[9] M. Kornhauser. A note on elastic surface deformation. *Journal of Applied Mechanics*, (18):251–252, 1951.

[10] R. Lewis and U. Olofsson. *Wheel-Rail Interface Handbook*. Woodhead Publishing, 2009. ISBN 978-1-84-569412-8.

[11] S.P. Timoshenko and J.N. Goodier. *Theory of Elasticity*. McGraw Hill, 1951.

[12] Willem van der Ham. *Tot gerief van de reiziger: vier eeuwen Amsterdam-Haarlem*. SDU, 1989. ISBN 978-9-01-206312-8.

[13] Xin Zhao. *Dynamic Wheel/Rail Rolling Contact at Singular Defects with Application to Squats*. PhD thesis, Delft University of Technology, 2012.